RUNNING HEAD: Discordant genomic and phenotypic clines

TITLE: When polymorphism and monomorphism meet: discordant genomic and phenotypic clines across a lizard contact zone

AUTHORS: Caroline M. Dong[1,2*], Claire A. McLean[1,2], Adam Elliott[1], Adnan Moussalli[2†], Devi Stuart-Fox[1†]

[1]School of BioSciences, The University of Melbourne, Parkville, Vic., Australia

[2]Sciences Department, Museums Victoria, Carlton Gardens, Vic., Australia

*Author for correspondence

†Joint last author

CORRESPONDING AUTHOR

Caroline M. Dong

School of BioSciences, The University of Melbourne, Parkville, Victoria 3010, Australia.

E-mail: caroline.dong@unimelb.edu.au

Abstract

Colour polymorphism can promote rapid evolution and speciation, particularly when populations differ in the number or composition of morphs. The tawny dragon, *Ctenophorus decresii*, is a compelling study system in which to examine evolutionary processes and outcomes when polymorphic and monomorphic lineages meet. The species comprises a northern lineage polymorphic for male throat coloration which lacks ultraviolet (UV) reflectance and a monomorphic southern lineage with UV-blue throats. We characterised genomic and phenotypic clines across the contact zone based on single nucleotide polymorphisms, the mitochondrial ND4 gene, and male colour traits, and concurrently assessed the phenotype of captive-bred F1 hybrids. Our results indicate that genomic introgression is asymmetric, with high frequencies of backcrossing to the northern but not southern lineage, accompanied by the prevalence of the northern mtDNA haplotype in hybrids. The clines for throat phenotype are abrupt and displaced to the south, relative to the genetic and dorsolateral phenotype clines. This suggests strong selection for the northern throat phenotype within the contact zone, particularly for the absence of ultraviolet reflectance, given the intermediate throat phenotype in captive-bred F1 hybrids. Our results demonstrate that a polymorphic sexual signal is the target of selection during incipient speciation and provide insight into the microevolutionary processes linking polymorphism and speciation.

Keywords: coloration, *Ctenophorus decresii*, introgression, speciation, reproductive isolation, ddRAD

Introduction

Colour polymorphism, the co-existence of multiple colour morphs within a single interbreeding population (Huxley, 1955), is possibly the best studied model of discrete intraspecific phenotypic variation. Recently, there has been great interest in the role of colour polymorphism in promoting rapid phenotypic evolution and speciation, particularly when populations differ in the number, type, and frequency of morphs (Corl, Davis, Kuchta, & Sinervo, 2010; Forsman, Ahnesjö, Caesar, & Karlsson, 2008; Gray & McKinnon, 2007; Hugall & Stuart-Fox, 2012; McLean & Stuart-Fox, 2014; West-Eberhard, 1986). However, we lack detailed studies on the microevolutionary processes linking colour polymorphism and speciation. In particular, the genomic and phenotypic consequences of secondary contact between polymorphic and monomorphic lineages remain unclear, especially where the monomorphic lineage represents a novel morph.

Colour morphs often represent alternative fitness optima that differ in a suite of co-adapted morphological, physiological, behavioural, and life-history traits, which allow multiple morphs to co-exist (Maynard-Smith 1996; Sinervo and Lively 1996; reviewed in McKinnon & Pierotti, 2010). These morph-specific trait combinations are generated by correlational selection and maintained by frequency-dependent selection, which together are expected to generate tight physical genetic linkage between associated loci or favour pleiotropic loci that control the expression of multiple traits to ensure optimal combinations (Sinervo & Svensson, 2002). Accordingly, morphs are predicted to be governed by few genes of major effect and indeed this has been substantiated in a number of systems (Küpper et al., 2016; Lank, Smith, Hanotte, Burke, & Cooke, 1995; McKinnon & Pierotti, 2010; O'Neill & Beard, 2010; Sinervo, Bleay, Adamopoulou, Inervo, & Leay, 2001; Wellenreuther, Svensson, & Hansson, 2014).

Based on the widespread importance of colour signals in reproductive isolation (Boughman, 2001; Jiggins, Naisbit, Coe, & Mallet, 2001; Mavárez et al., 2006; Sætre et al., 1997; Seehausen et al., 2008) and the underlying genetic architecture of polymorphism (Sinervo & Svensson, 2002), there is expected to be a high probability of incompatibility during secondary contact between populations that differ in morph number, type, or frequency. Gene flow may result in the breakdown of adaptive genetic correlations and generate genetic incompatibilities between morphs (Pryke & Griffith, 2009). More generally, incompatibilities may arise when coadapted alleles are brought together for the first time in hybrids (Dobzhansky-Muller incompatibilities; Dobzhansky, 1937; Muller, 1942) or when coadapted nuclear and organelle (e.g. mitochondria and chloroplast) genomes that evolved in allopatry are disrupted (cytonuclear incompatibilities; Burton and Barreto 2012; Hill 2015). Further, a divergence in sexual phenotypic characteristics may also be accompanied by behavioural incompatibilities in mating preferences resulting in restricted gene flow and/or selection against hybrids. These phenotypic and genetic incompatibilities together may facilitate the process of speciation between populations which differ in morph frequencies and/or composition.

Here, we investigate the outcome of contemporary contact between colour polymorphic and monomorphic lineages of *Ctenophorus decresii* (tawny dragon*;* Duméril & Bibron, 1837) that differ in both morph number and type. The species comprises two phylogeographically structured lineages which differ in male dorsolateral and throat coloration (Houston 1974; McLean et al. 2014b; Figures 1 and 2a). The polymorphic northern lineage has four discrete male throat colour morphs that are present in all populations and reflect little to no ultraviolet (UV): orange, yellow, yellow with orange centre, and grey (Teasdale et al. 2013; Figure 1a). The black dorsolateral stripe is relatively straight-edged and

continuous, sometimes with one distinct blotch near the neck, and with yellow/orange coloration terminating just behind the shoulder (McLean, Moussalli, Sass, & Stuart-Fox, 2013). By contrast, southern lineage males have blue throat coloration with a strong UV reflectance peak, representing a novel morph (Figures 1b; McLean et al. 2014b). The black dorsolateral stripe is discontinuous with two distinct blotches near the neck and coloration terminating mid-body (McLean et al., 2013). The throat colour polymorphism is likely to have evolved in *C. decresii* and then was subsequently lost in the southern lineage, thereby facilitating the evolution and fixation of the novel blue morph (McLean, Stuart-Fox, et al., 2014). Genetic divergence between the northern and southern lineages (3.7% net sequence divergence in mtDNA) is consistent with range contraction to allopatric refugia during glacial-interglacial Pleistocene cycles (Byrne, 2008; McLean, Stuart-Fox, et al., 2014), where differing site-specific selective pressures may have led to the evolution of divergent phenotypes. A small number of genetically admixed individuals have been identified where the lineages meet geographically, suggesting that subsequent post-glacial range expansion has resulted in a secondary contact zone (McLean, Stuart-Fox, et al., 2014).

This is a compelling study system to explore the evolutionary consequences of secondary contact between colour polymorphic and monomorphic lineages because their biology is well-characterised. *C. decresii* is sexually dichromatic: females have cream coloured throats with a cryptic dorsal phenotype and males have bright throats with lineage-specific dorsolateral patterning and coloration. Throat and dorsolateral coloration are important intraspecific sexual signals, which are emphasised during complex movement-based territorial and courtship displays involving head-bobbing and push-ups (Gibbons, 1977, 1979; Osborne, Umbers, Backwell, & Keogh, 2012; Ramos & Peters, 2016; Stuart-Fox & Johnston, 2005). The four morphs of the northern lineage employ alternative behavioural

strategies (Yewers, Pryke, & Stuart-Fox, 2016) corresponding to differing hormonal profiles (Yewers, Jessop, & Stuart-Fox, 2017), and are associated with MHC supertypes (Hacking, Stuart-Fox, Godfrey, & Gardner, 2018). Male throat coloration develops at sexual maturity (ca. 18 months), is fixed for life, and autosomally inherited. The discrete polymorphism is likely controlled by two independently segregating loci, though the extent of orange or yellow within morphs behaves as a quantitative (polygenic) trait (Rankin, McLean, Kemp, & Stuart-Fox, 2016).

We used a method of double digest restriction-site associated DNA sequencing to identify single nucleotide polymorphisms (SNPs), sequenced the mitochondrial ND4 gene, and characterised male throat and dorsolateral phenotype across a naturally occurring contact zone between the polymorphic northern and monomorphic southern lineages. Using geographic cline analysis, we compared the frequency of these genetic and phenotypic traits along a transect through the contact zone from pure southern to pure northern populations. Furthermore, we conducted captive-breeding to investigate F1 hybrid phenotype independent of exogenous selection. Specifically, we examined i) the geographic extent of hybridisation, ii) whether contact is very recent or several generations old, iii) whether hybridisation is bidirectional or asymmetric, and iv) whether there is evidence of selection on phenotype. We predicted that selection on throat coloration to maintain the northern polymorphism should result in steeper and narrower clines compared to SNP and dorsolateral phenotype clines.

Materials and Methods

Field sampling

Ctenophorus decresii is a small [snout-vent-length (SVL) ≤ 90 mm] diurnal rock-dwelling agamid endemic to South Australia. The northern lineage occurs in the Flinders and Olary Ranges whereas the southern lineage occurs in the Mount Lofty Ranges, Fleurieu Peninsula, and on Kangaroo Island (Figure 2b). The contact zone is found in an area of relatively low-lying grassland between the rocky ranges of the parental lineages, coinciding with a change from relatively temperate to more semiarid conditions (Houston 1974; McLean et al. 2014b). Our sampling design aimed to capture the full geographic range of the species (Figure 2b, Table S1) to reaffirm previously described genetic divergence based on multi-loci sequence data and microsatellites (McLean, Stuart-Fox, et al., 2014). To extend this previous work we intensively sampled 14 sites along a north-south 160 km transect through the contact zone (Figure 2c, Table S2). As the geographic extent of hybridisation was initially unknown, the transect was anchored on either end by two genetically pure southern (sites 1 – 2) and pure northern (sites 13 – 14) populations. Lizards were captured by noosing (telescopic pole and noose made of fishing line) or by hand and released at the site of capture following data collection. A genetic sample (blood or tail tip stored in 99% ethanol at -20°C) and phenotypic data (described below) were taken from each individual. We focused on collecting data from adult males (SVL ≥ 65 mm) and collected genetic samples from females opportunistically. In total, our dataset comprised 234 genetic samples from across the species range (Table S1). This included 152 genetic samples and phenotypic data from up to 233 males along the contact zone transect, depending on trait (Table S2).

SNP discovery

Genomic DNA was isolated and purified from blood or tissue using either an E.Z.N.A. Tissue DNA Kit (Omega Bio-tek, Norcross, GA, USA) or a GenCatch Blood and Tissue Genomic Mini-Prep Kit (Epoch Life Sciences, Sugar Land, TX, USA). After quantification

158 using a QIAxpert (Qiagen), we sent between 500 and 1000 ng of DNA at a final concentration
159 of between 50 and 100 ng/uL to Diversity Arrays Technology (Bruce, ACT, Australia) for
160 SNP genotyping using DarTseq, a genome complexity reduction method similar to double
161 digest restriction-site associated DNA (ddRAD) sequencing protocol. Protocols are described
162 in detail for broad applications in Kilian et al., 2012 and specifically for the genus
163 *Ctenophorus* in Melville et al., 2017. Briefly, genomic DNA was digested with two restriction
164 endonucleases (PstI/HpaII), PCR amplified (1 min at 94°C; 30 cycles of 94°C for 20 s, 58°C
165 for 30 s, 72°C for 45 s; final extension at 72°C for 7 min), and sequenced on an Illumina
166 HiSeq2500. 'High-density' DArTseq SNP arrays use 2,500,000 (±7%) reads per sample in
167 marker calling. Two technical replicates of each DNA sample were genotyped to assess
168 reproducibility. DArT analysis pipelines and a calling algorithm (DArTsoft14) were used to
169 process sequences into a matrix of SNP loci. As reference genomes, we used the *C. decresii*
170 draft genome (McLean, Stuart-Fox, and Moussalli, unpublished data) and the fully annotated
171 central bearded dragon genome (*Pogona vitticeps;* Georges et al., 2015). In total, we obtained
172 172,893 SNPs from 234 individuals with 41.54% missing data. Using the R package *dartR*
173 (v1.1.6, Gruber et al. 2018), we filtered this dataset conservatively with thresholds of 100%
174 reproducibility, ≤1% missing data per locus, ≤10% missing data per individual, and also
175 removed loci that deviated from Hardy-Weinberg Equilibrium ($P < 0.05$). This resulted in a
176 dataset of 1,333 SNPs from 230 individuals with 0.26% missing data.

177 *Mitochondrial DNA*

178 We sequenced an 850 base-pair region of the mitochondrial genome which included
179 the NADH dehydrogenase subunit four (ND4), and tRNAhis, tRNAser and tRNAleu regions
180 using the primers ND4F (Forstner, Davis, & Arèvalo, 1995) and tRNA-Leu (Scott & Keogh,
181 2000) for a subset of 74 individuals from sites across the contact zone transect (Table S1).

PCR was performed in 25µL reactions containing 12.5µL GoTaq Hot Start Master Mix (Promega, Madison, Wisconsin, USA), 1µL forward and reverse primer (10µM), and 1µL DNA. Cycling conditions included an initial denaturation (95°C for 4 min) followed by 35 cycles total of denaturation (95°C for 45 s), annealing (10 and 25 cycles of 45 s at 56°C and 54°C, respectively), and extension (72°C for 1.5 min) with a final extension period of 72°C for 7 min (McLean, Stuart-Fox, et al., 2014). PCR products were submitted to the Australian Genome Research Facility (Melbourne, Victoria, AUS) for purification and forward and reverse sequencing on an Applied Biosystems 3730xl DNA Analyzer. Sequences were edited and aligned with additional ND4 sequences of northern and southern lineage *C. decresii* (McLean, Stuart-Fox, et al., 2014) in Geneious (v6.1.7; Kearse et al. 2012). Haplotype networks were constructed using the statistical parsimony algorithms of TCS (v1.21; Clement et al. 2000).

Quantifying population structure and admixture

We examined genome-wide patterns of divergence using the Bayesian model-based clustering approach implemented in STRUCTURE (v2.3.4; Pritchard, Stephens, & Donnelly, 2000). After an initial burn-in of 500,000 Markov chain Monte Carlo (MCMC) generations, we ran 500,000 generations with 10 independent replicates for K values ranging from 1 to 5 under the "admixture" model with correlated allele frequencies and prior population information, all other parameters were kept at default, and convergence of runs was visually assessed. We used STRUCTUREHARVESTER (Earl & VonHoldt, 2012) to identify the optimum value of K for our dataset and summarised results across the selected value of K using CLUMPP (v1.1.2; Jakobsson & Rosenberg, 2007). We used the Bayesian estimation of the *q*-value (proportion of an individual's genome inherited from each parental population) with 95% confidence intervals (CI) as a hybrid index. Individuals were identified as pure

206 parentals or putative hybrids based on their hybrid index and 95% CI: an individual was
207 classified as parentals if $0.1 \geq q \geq 0.9$ or of mixed ancestry if $0.1 < q < 0.9$.

208 We used previously identified population groups within each parental lineage to
209 further examine population structure (North: Northern Flinders Ranges [NFR], Southern
210 Flinders Ranges [SFR], Olary Ranges [OR]; South: Mainland South [MS], Kangaroo Island
211 [KI]; McLean et al. 2014b) and Contact Zone (CZ). We calculated expected and observed
212 heterozygosity, the number of alleles and allelic richness, estimated population pairwise F_{ST},
213 and the inbreeding coefficient (F) for each population using the R packages *dartR* (v1.1.6;
214 Gruber et al. 2018) and *adegenet* (v2.1.1; Jombart & Ahmed, 2011). We then performed a
215 principal coordinate analysis (PCoA) using *dartR* to visualize pairwise genetic distances
216 between individuals.

217 *Hybrid classification*

218 We identified 15 diagnostic loci (fixed for alternate alleles between lineages) which
219 had allele frequencies of ≥ 0.90 and ≤ 0.1 in parental populations using the R package *dartR*
220 (v1.1.6, Gruber et al. 2018) for hybrid classification analysis. We used the program
221 NEWHYBRIDS (v1.1 Anderson & Thompson, 2002) to determine the probability that
222 individuals within the contact zone belonged to one of the six genotypic classes resulting from
223 the first two generations of hybridisation: parental forms (P1 and P2), F1 (P1 × P2), F2 (F1 ×
224 F1), and backcrossed (F1 × P1/P2). A total of 500,000 MCMC generations were run after an
225 initial burn-in of 100,000 generations with uniform priors for alleles and mixing proportions.
226 We ran this analysis five times and averaged probabilities across runs. Although it is not
227 always possible to unambiguously assign individuals into discrete classes due to the
228 continuum that may be found in wild populations, classification may be suggestive of

229 situations where contact is very recent or where F1 hybrids are infertile based on the absence
230 of F2 hybrids and backcrosses, or where contact is several generations old based on the
231 absence of pure parentals and F1 hybrids.

232 *Captive-breeding and testosterone-induced expression of colour traits*

233 To evaluate F1 hybrid phenotype independent of extrinsic selection pressures, we
234 conducted captive breeding using 36 pure southern lineage individuals (female = 17, male =
235 19) collected from cline site 1 (southernmost site, longitude: 139.103°, latitude: -33.443°) and
236 41 pure northern lineage individuals (female = 20, male = 21) from cline site 14
237 (northernmost site, longitude: 139.103°, latitude: -33.443°; Table S2, Figure 2c) to produce
238 reciprocal cross hybrids, in addition to pure lineage offspring for comparison. Male and
239 female pairs were housed together until the female was visibly gravid, eggs were collected
240 following oviposition and incubated until hatching. Offspring were housed individually and
241 reared under laboratory conditions (total = 138; southern = 11, northern = 54, hybrids = 73).
242 We genotyped adults and offspring at five microsatellite loci (Am41, Cp10, Ctde45, Ctde05,
243 Ctde12; Schwartz et al. 2007; McLean et al. 2014b) and confirmed paternity using a
244 maximum likelihood approach in CERVUS (v3.0.7; Kalinowski, Taper, & Marshall, 2007;
245 Marshall, Slate, Kruuk, & Pemberton, 1998). For all offspring, we induced throat colour
246 expression by artificially elevating testosterone levels at nine months of age in both sexes
247 (female = 64, male = 74; supplemental information). Females can be induced to express
248 discrete throat morphs found in males using testosterone (Rankin & Stuart-Fox, 2015), but
249 dorsolateral patterning and coloration remain cryptic therefore dorsolateral phenotype was
250 analysed only for male offspring. See supplemental information for full details of breeding,
251 rearing, genotyping, and throat colour expression procedures.

252 *Analysis of phenotypic data*

253 To characterise the phenotype of wild-caught males and captive-bred F1 hybrids, we
254 took standardised ventral (i.e. throat) and dorsal photographs and spectral reflectance
255 measurements of throat colours. Photographs were taken using a Canon EOS 600D digital
256 camera, saved in raw format, and included an Xrite colour standard and ruler for scale
257 (Stevens, Párraga, Cuthill, Partridge, & Troscianko, 2007). Images were converted to 8-bit tiff
258 files using Digital Photo Professional (v4.5.0.0; Canon Inc.), linearised with respect to
259 radiance, and equalised against a grey standard (Stevens et al. 2007; as per Smith et al. 2016).
260 We then performed a segmentation analysis (detailed in Teasdale et al., 2013) to extract the
261 proportion of each colour present on the throat (i.e. orange, yellow, blue), classify throats into
262 existing morphs (orange, yellow, orange-yellow, grey, or blue), and to quantify the proportion
263 of orange and yellow colouration present on the head and neck from dorsal photographs.
264 Image analysis was conducted using custom code written in MATLAB (The MathWorks,
265 Inc., Natick, MA, USA; see Teasdale et al., 2013). We also manually quantified the number
266 of distinct breaks in the dorsolateral stripe near the neck by visually inspecting all
267 photographs of the dorsal region.

268 We took spectral reflectance measurements (300 – 700 nm) to quantify variation in
269 UV reflectance, using an Ocean Optics (Dunedin, FL, USA) Jaz portable spectrometer. The
270 probe was held at a constant angle (45°) and distance from the surface of the skin.
271 Measurements were expressed relative to a Spectralon 99% diffuse white reflectance standard
272 (Labsphere, Inc., North Sutton, NH, USA). At least two measurements were taken of each
273 colour present on the throat, then averaged. For each throat colour patch, we estimated the
274 receptor quantum catch (QC), the stimulation of retinal photoreceptors, for the violet to UV
275 wavelength sensitive (UVS) photoreceptor because we were specifically interested in the

diagnostic UV-blue component of throat coloration. The R package *pavo* (v1.3.1; Maia, Gruson, Endler, & White, 2018) was used to process reflectance measurements.

We performed principal component analyses (PCA) to explore variation in throat coloration variables (proportion of orange, proportion of yellow, proportion of blue) and dorsolateral phenotype variables (proportion orange, proportion of yellow, breaks in the dorsolateral stripe) in the R package *FactoMineR* (v1.4.1; Le, Josse, & Husson, 2008). In each, the lineages were differentiated along the first dimension (PC1) and this was used to collapse variables into a single measure of overall phenotype and retained for use in subsequent cline analyses. The quantum catch of the UV sensitive photoreceptor (QC_{UVS}) was used singly in cline analyses to assess its frequency across the contact zone independent of throat colour morph. Due to missing data, 204 individuals were used in throat phenotype analyses whereas 233 individuals were used in dorsolateral phenotype analyses. Linear discriminant analyses were performed on pure individuals in the R package *MASS* (v7.3.50; Ripley, 2002) using all throat phenotype variables (proportion of orange, yellow, and blue, and QC_{UVS}) and dorsolateral phenotype variables as independent variables.

Geographic cline analysis

We used the R package *HZAR* (v0.2-5, Derryberry, Derryberry, Maley, & Brumfield, 2014) to fit a series of equilibrium geographic cline models (Gay, Crochet, Bell, & Lenormand, 2008; Szymura & Barton, 1986; Szymura & Barton, 1991) to both the molecular and phenotypic datasets, and in all cases using 1,000,000 MCMC generations following an initial burn-in of 100,000 generations. Specifically, we estimated cline models for the hybrid index (H_{Index}; Bayesian *q*-value based on 1,333 loci), mtDNA haplotype frequencies, quantum

298 catch of the UV wavelength sensitive receptor (QC_{UVS}), PC1 for throat coloration (T_{PC1}), and
299 PC1 for dorsolateral phenotype (D_{PC1}).

300 *HZAR* uses logistic regression equations to fit sigmoidal clines in a maximum-
301 likelihood framework and describes cline centre (*c*) as the position where estimated trait
302 frequency is 0.5 and width (*w*) as 1/slope at the cline centre. For molecular clines, we
303 compared 15 models that varied in the fitting of trait interval (*p*; minimum and maximum
304 frequencies at tails; fixed at 0 and 1, observed values, estimated values) and exponential
305 decay tails (none, right only, left only, mirrored, both estimated separately). These 15 models
306 were compared to an additional null model. For phenotypic trait data we compared models
307 that varied in the fitting of exponential decay tails (none, right only, left only, mirrored, both
308 estimated separately) and estimated mean and variance on the ends and in the centre. All
309 models estimated cline centre and width as well as tail parameters if applicable (δ, distance
310 from the centre to the tail; τ, tail slope). QC_{UVS} and T_{PC1} were normalised to values between 0
311 and 1 for plotting purposes.

312 To address model selection uncertainty, we conducted model averaging in an Akaike's
313 information criterion (AIC) framework. We calculated the Akaike weight (AIC*w*), a value
314 between 0 and 1 which can be interpreted as the probability of being the best approximating
315 model (Burnham & Anderson, 2002). Models were then ranked by AIC*w* downwards until the
316 cumulative AIC*w* reached 0.95 to attain a 95% confidence set of best-ranked models (Lukacs,
317 Burnham, & Anderson, 2010; Symonds & Moussalli, 2011). We recalculated the AIC*w* of
318 models in the 95% confidence set and used those to calculate the model-averaged estimate of
319 parameters (e.g. centre and width). We produced model-averaged clines by first multiplying
320 the estimate for a given distance interval by the AIC*w*. This was done for each model within
321 the 95% confident set of models. The AIC model averaged estimate was then obtained by

summing up weighted estimates for each distance interval. Similarly, we multiplied the minimum and maximum estimate bounds by the AIC*w*, followed by summation to represent the credible region. Finally, the coincidence of cline centres was assessed by comparing model-averaged maximum-likelihood derived CIs (two log-likelihood unit support limits) of cline centres, with non-overlapping CIs considered statistically supported differences. Akaike weights were calculated using the R package *MuMIn* (v1.43.6; Bartoń 2018).

Results

Population structure and admixture

We found distinct population structure across the species range with the most prominent divide between the northern and southern lineages and evidence for the presence of hybrids in the contact zone. Based on the STRUCTURE analysis, only two clusters were identified, corresponding to the major split between the northern and southern lineages (Figure 2d, Table S3). The *q*-values ranged from 0.999 (pure southern) to 0.001 (pure northern). Across the contact zone transect, individuals from the southernmost sites 1 – 2 had a high probability of belonging to the southern genetic cluster ($q \geq 0.90$; mean ± SD = 0.99 ± 0.02) with the exception of two admixed individuals ($q = 0.81$ and 0.57). All individuals from the northernmost sites 9 – 14 had a high probability of belonging to the northern genetic cluster ($q \leq 0.10$; mean ± SD = 0.04 ± 0.03). Hybrids were identified within sites 3 – 8 where all individuals were of mixed ancestry and exhibited a highly skewed continuum of *q*-values ranging from 0.53 to 0.11. These sites will hereinafter be referred to as 'the contact zone', encompassing a distance of approximately 22.5 km. We also identified a density trough of approximately 12 km between sites 2 and 3 (Figures 2c–d) across which the genotype changes

345 abruptly and multi-year surveys recovered no individuals. With the exception of two
346 individuals at site 3, all admixed individuals in sites 3 – 13 had northern lineage mtDNA
347 haplotypes. The southern lineage mtDNA haplotype was fixed in sites 1 – 2, including the
348 only two admixed individuals identified in the geographic range of the southern lineage
349 (Figure S1).

350 The first axis of the PCoA constructed from 1,333 loci clustered all populations into
351 two major groups corresponding to the northern and southern lineage (variance explained =
352 19.4%; Figure 3). We found evidence for the presence of hybrids along this axis, with hybrids
353 clustered more closely to northern lineage Olary Ranges (OR) population. Population
354 pairwise measures of F_{ST} between the contact zone and northern lineage OR/SFR/NFR
355 populations (F_{ST} range: 0.058 – 0.216; Table S4) were lower relative to measures of F_{ST}
356 between the contact zone and southern lineage MS/KI populations (F_{ST} range: 0.203 – 0.293).
357 The contact zone had the lowest inbreeding coefficient (F = 0.095) and the highest level of
358 heterozygosity (H_{exp} = 0.084, H_{obs} = 0.079) relative to parental populations, with very similar
359 allelic number and richness to the OR population (Table 1). The second PCoA axis (variance
360 explained = 3.5%) showed population structure within each lineage, with the Northern
361 Flinders Ranges (NFR) and Kangaroo Island (KI) populations showing differentiation from
362 other populations of their respective lineages (F_{ST} = 0.571). This can likely be attributed to the
363 fact that each represents the northernmost and southernmost populations of their lineages, and
364 KI is an insular population.

365 *Hybrid classification*

366 We found a strong bias in genetic introgression with admixed individuals being
367 predominantly backcrossed with the northern lineage. Of individuals within the contact zone,

368 35% had intermediate *q*-values ($0.4 < q < 0.6$) and a large proportion (65%) had *q*-values
369 between 0.39 and 0.10 suggestive of backcrossing. We found fewer individuals with
370 intermediate *q*-values using diagnostic loci (13.75%) with a larger proportion of backcrossed
371 individuals (86.25%). NEWHYBRIDS classified 88.75% of individuals in the contact zone to
372 one of the six classes with a posterior probability (PP) of $\geq$ 75%. Additionally, 18.75% of
373 individuals were classified as pure northern (P1), 22.5% as F2 hybrids, and 47.5% as
374 backcrosses to the northern lineage (B1). We did not recover any F1 hybrids and posterior
375 probabilities of individuals being classified as backcrosses to the southern lineage were
376 uniformly low (PP $\leq$ 13.31%). Of the two admixed individuals found in the geographic range
377 of the southern lineage, one was classified as F2 and the other was unable to be classified (PP
378 $\leq$ 75%). Individuals unable to be confidently classified likely represent the continuum present
379 in wild populations, unsuited for discrete classification, and difficult to distinguish even with
380 many diagnostic markers (Boecklen & Howard, 1997; Vähä & Primmer, 2006).

381 *Hybrid throat and dorsolateral phenotypes*

382 The throat phenotype of wild-caught hybrid males was more similar to that of the
383 northern lineage, exhibiting all four northern throat colour morphs with uniformly low levels
384 of UV reflectance. Linear discriminant analyses (LDA) on throat variables showed the
385 northern and southern lineages strongly differentiated along LD1 which was driven primarily
386 by the proportion of blue and secondarily by QC_{UVS} and the proportion of orange (variance
387 explained = 99.8%; Figure 4a, Table S5). The 95% confidence ellipses drawn for the throat
388 phenotypes of northern and hybrid males overlie each other. The large majority of hybrid
389 throats cluster with northern throats. Blue coloration was not detected on the throats of pure
390 northern males. A degree of blue coloration ($\geq$ 5% blue pixels in segmentation analysis),
391 however, was found on a portion of hybrid throats of each morph: grey (47.4%, N = 19),

392 orange (5.2%, N = 39), orange-yellow (6.7%, N = 15), yellow (11.8%, N = 17; Figure 5a).
393 The throat phenotype of the two hybrid individuals found in the range of the southern lineage
394 had larger proportions of blue coloration on the throat relative to other hybrids.

395 In contrast to wild-caught hybrid throats, captive-bred F1 hybrid throat phenotype was
396 more intermediate and exhibited a wide range of UV reflectance levels varying from those
397 characteristic of the northern to southern lineages. Linear discriminant analysis on throat
398 variables of captive-bred F1 hybrids showed strong differentiation between lineages along
399 LD1 driven primarily by QC_{UVS} and secondarily by the proportions of blue and yellow
400 (variance explained = 88.0%; Figure 4b, Table S5). The 95% confidence ellipse drawn for
401 hybrid throats overlaps those of both northern and southern throats to a similar extent. Results
402 were essentially unchanged when considering hybrids sired by a northern or southern male
403 and by offspring sex. Similar to wild hybrids, all four northern throat colour morphs were
404 recovered in captive-bred hybrids, and all but the orange-yellow morph had a proportion of
405 individuals with a blue component: grey (32.3%, N = 31), orange (18.5%, N = 27), orange-
406 yellow (0%, N = 2), yellow (8.3%, N = 12; Figure 5b). Although the artificial elevation of
407 testosterone levels has been shown to induce the expression of northern throat colour morphs
408 in juveniles and females (Rankin et al., 2016; Rankin & Stuart-Fox, 2015), we found that it
409 did not comparably induce the expression of the blue throat colour morph in all pure southern
410 offspring. Therefore, the presence of blue coloration on F1 hybrid offspring throats may have
411 been underestimated.

412 Dorsolateral phenotype in both wild-caught and captive-bred hybrids is intermediate
413 between the lineages (Figures 4c–d). Within the contact zone, differentiation between lineages
414 along LD1 is driven primarily by the number of breaks in the dorsolateral stripe and
415 proportion of orange (Table S5). The 95% confidence ellipses drawn for the dorsolateral

phenotypes of hybrids and northern males overlap incompletely, likely reflecting the high frequencies of backcrossing to the northern lineage. In captive-bred hybrids, comparable results were found with differentiation driven by breaks in the lateral stripe (Table S5) and the 95% confidence ellipse for hybrid dorsolateral phenotype overlaps those of both northern and southern dorsolateral phenotypes.

Geographic clines

Model-averaged clines for mtDNA and throat phenotype (QC_{UVS} and T_{PC1}) exhibited relatively narrower clines with abrupt transitions suggesting selection on these traits, compared to clines for the hybrid index (H_{Index}) and dorsolateral phenotype (D_{PC1}; Table 2). The best-fitting clines for the hybrid index and mtDNA had coincident centres with overlapping CIs but showed discordance in slope where the mtDNA cline was significantly narrower (H_{Index}: c = 28.41 km, w = 29.77 km; mtDNA: c = 27.78 km, w = 0.64 km; Figure 6a–b). The cline fitted for the dorsolateral phenotype (c = 23.02 km, w = 13.97) was coincident with that of the hybrid index (Figure 6c). Clines for throat phenotype (QC_{UVS} and T_{PC1}) were similar in centre and width to each other (QC_{UVS}: c = 15.90 km, w = 8.48 km; T_{PC1}: c = 15.38 km, w = 3.22 km; Figure 6d), their centres were displaced by 12.51 and 13.03 km to the south from the hybrid index cline centre and do not have overlapping CIs with the hybrid index cline. See Table S6 for full details of cline models in the AIC 95% confidence set for each trait.

Discussion

Evaluating the evolutionary outcomes of secondary contact between lineages that differ in morph composition can provide valuable insights into the role of polymorphism in

speciation. We characterised genomic and phenotypic patterns across the contact zone between colour polymorphic and monomorphic lineages of *C. decresii* and concurrently measured the phenotype of captive-bred F1 hybrids. We found that the contact zone is geographically narrow and appears to be several generations old with no parental forms or F1 hybrids present in the genetic centre. Further, we found evidence of asymmetric genomic introgression with hybrid backcrossing almost exclusively to the northern lineage, which suggests that hybridisation between the lineages is not ongoing. This, accompanied by the prevalence of the northern lineage mtDNA haplotype across the contact zone, suggests differing levels of selection against particular recombinants. Dorsolateral phenotype across the contact zone appeared to be the result of genetic admixture whereas there was evidence of selection for the northern throat polymorphism within the contact zone. We found all four northern throat morphs present with low UV reflectance in wild-caught hybrids, contrasting with highly variable and intermediate levels of UV reflectance in captive-bred hybrids.

Multiple lines of evidence suggest reproductive incompatibilities between the divergent lineages of *C. decresii*. We found a geographically narrow area of admixture relative to the parental ranges, with hybrids backcrossing almost exclusively to the northern lineage. The restricted gene flow to the southern lineage is associated with an approximately 12 km density trough (Figures 3b–c) where it appears that *C. decresii* populations either occur in levels below human detection or do not currently exist despite continuous rocky habitat with no obvious barriers to dispersal. Our findings suggest that the density trough is a result of intrinsic genomic incompatibilities rather than extrinsic factors preventing dispersal and backcrossing to the southern lineage. The narrower and more abrupt transition exhibited by the mtDNA cline relative to the hybrid index and the rarity of admixed individuals containing the southern mtDNA haplotype provide further evidence of selection against particular

463 recombinants across the contact zone. Captive breeding experiments show no significant
464 prezygotic barriers to the formation of F1 hybrids with either parental mtDNA haplotype
465 (Dong, Rankin, McLean, & Stuart-Fox, unpublished data), although their reproductive
466 viability is unknown. However, stronger incompatibilities and hybrid breakdown are more
467 frequently seen in F2 and later generation hybrids during the early stages of divergence. This
468 has been described extensively for both Dobzhansky-Muller incompatibilities (reviewed in
469 Coyne & Orr, 2004) and for cytonuclear incompatibilities (Ellison & Burton, 2008; Fishman
470 & Willis, 2006; Meiklejohn et al., 2013; Niehusis, Judson, & Gadau, 2008). Ultimately,
471 backcrossing to the southern lineage, regardless of mtDNA haplotype, may result in offspring
472 that are inviable, infertile, or suffer greatly reduced fitness.

473 We found evidence that the northern throat phenotype is selectively favoured within
474 the contact zone, in terms of both discrete throat morphs and UV reflectance. Although throat
475 and dorsolateral coloration are both sexually dichromatic traits, the throat phenotype clines
476 were both displaced to the southern end of the contact zone, with the northern throat
477 phenotype prevalent in hybrids. By contrast, the dorsolateral coloration cline was more
478 concordant with the genetic cline. Selection has been shown to drive the rapid spread of an
479 advantageous trait/phenotype across contact zones, and in some cases into the other parental
480 lineage (Baldassarre, White, Karubian, & Webster, 2014; Pardo-Diaz et al., 2012; Stein & Uy,
481 2006; While et al., 2015). We did not detect the loss of any northern throat morphs across the
482 contact zone or in F1 hybrids, indicating that co-adapted trait complexes of the northern
483 polymorphism are stable despite genetic disruption. Although hybrid throats were objectively
484 and confidently classified into discrete northern throat morphs, we observed a proportion of
485 each morph which exhibited a degree of intermediate nature where an area of blue coloration
486 was present. There was a notably higher proportion of grey morphs which had blue coloration

present. This may be due to the similar mechanism by which grey and blue skin are produced in *C. decresii*, both from melanin pigments in melanophores with blue skin incorporating an additional structural component produced from guanine crystals in iridophores (McLean, Lutz, Rankin, Stuart-Fox, & Moussalli, 2017). Nevertheless, we did not detect any hybrid throats that exhibited a true southern throat phenotype with both predominantly blue throat coloration and a high level of UV reflectance. This, in addition to the wide range of UV reflectance found in captive-bred F1 hybrids, points toward the uncoupling of blue coloration and UV reflectance in hybrids driven by stronger negative sexual selection against UV reflectance as a singular trait.

Selection for the northern throat polymorphism could be driven by mating behaviour which evolved via reinforcement and/or microhabitat characteristics. Mate preference trials with captive *C. decresii* predict a greater frequency of mating between southern females with northern males than the reciprocal combination (McLean, Bartle, Dong, Rankin, & Stuart-Fox, submitted). This contrasts with patterns observed within the contact zone, indicating that prezygotic barriers between lineages have not evolved in allopatry. However, prezygotic barriers are expected to form in the contact zone because postzygotic barriers (inferred from low frequency of hybrids backcrossed to the south) should select for the formation of prezygotic barriers to prevent maladaptive hybridisation (i.e. reinforcement). Extrinsic factors could also contribute to the northern throat phenotype having a competitive advantage in the contact zone, for example, due to a relatively higher conspicuousness to conspecifics. Throat coloration of each lineage is more conspicuous against the predominant background colours of native lichen in their respective ranges (McLean, Moussalli, & Stuart-Fox, 2014). Within the contact zone, lichen coloration is similar to that found in the range of the northern lineage, predominantly pale green. Therefore, sexual selection may operate through male-male

511 interactions or female choice to result in a reproductive advantage of the northern throat
512 phenotype as a more conspicuous and detectable visual signal. In contrast, the dorsolateral
513 phenotype cline indicates that it is not under similarly strong selection and appears to play a
514 lesser role in reproductive isolation in sympatry. Male dorsolateral coloration may be
515 constrained as it is under both sexual and natural selection because of its dual function as a
516 intraspecific signal and in minimising conspicuousness to predators against native lichen
517 (McLean, Moussalli, et al., 2014; Ramos & Peters, 2016).

518 *Conclusions*

519 In summary, our data indicate that sexual signal divergence and intrinsic genetic
520 incompatibilities play an important role in restricting gene flow between polymorphic and
521 monomorphic lineages of *C. decresii*. Our results suggest that the reciprocally monophyletic
522 lineages remain distinct in the face of gene flow with evidence of isolating barriers. Thus,
523 consideration should be given towards elevating the lineages to species status based on
524 genetic and phenotypic divergence with restricted gene flow. Our findings also demonstrate
525 that a polymorphic sexual signal is the target of selection during incipient speciation. The
526 stability of the northern polymorphism despite genetic disruption is consistent with the
527 theoretical genetic architecture of colour polymorphism and correlated traits, namely control
528 by pleiotropic or tightly linked genes. Taken together, these results are consistent with the
529 view that polymorphism can promote speciation.

530

531

Acknowledgements

This study was funded by the Australian Research Council (grant nos. DP150101048 and DP1092908) to D.S-F., the Holsworth Wildlife Endowment to C.M.D. and C.A.M., Alfred Nicholas Fellowship and Nature Foundation South Australia to C.A.M. We thank Madeleine Yewers, Steven Mesis, and Jessica Borgh for assistance in the field; Katrina Rankin for assistance with captive animal husbandry; Anne Auslebrook for assistance with image analysis; private landowners for kindly allowing access to their property for field sampling; and South Australian Museum for providing tissue samples. Ben Phillips provided constructive comments on an earlier draft. Data collection was conducted with permits from the Department of Environment, Water and Natural Resources, South Australia (permit nos. E25861-1 and Q26428-3), the Department of Environment, Land, Water and Planning, Victoria (permit nos. 10007000 and 10007751) and with approval by the University of Melbourne Animals Ethics Committee (approval nos. 1011760.1 and 1413220.4), the Wildlife Ethics Committee of South Australia (approval nos. 18/2010 and 25/2015).

Author Contributions

All authors contributed to study design and field sampling. C.M.D. and C.A.M. performed laboratory work. C.M.D. conducted data analyses and drafted the manuscript, C.A.M, A.M. and D.S-F provided input on analyses and interpretation. All authors read and approved the final manuscript.

553 **References**

554 Anderson, E. C., & Thompson, E. A. (2002). A model-based method for identifying species
555 hybrids using multilocus genetic data. *Genetics*, *160*(3), 1217–1229.

556 Baldassarre, D. T., White, T. A., Karubian, J., & Webster, M. S. (2014). Genomic and
557 morphological analysis of a semipermeable avian hybrid zone suggests asymmetrical
558 introgression of a sexual signal. *Evolution*, *68*(9), 2644–2657. doi:10.1111/evo.12457

559 Bartoń, K. (2018). MuMIn: Multi-Model Inference. R package version 1.42.1.
560 https://CRAN.R-project.org/package=MuMIn.

561 Boecklen, W. J., & Howard, D. J. (1997). Genetic analysis of hybrid zones: numbers of
562 markers and power of resolution. *Ecology*, *78*(8), 2611–2616. doi:10.1890/0012-
563 9658(1997)078[2611:gaohzn]2.0.CO;2

564 Boughman, J. W. (2001). Divergent sexual selection enhances reproductive isolation in
565 sticklebacks. *Nature*, *411*(6840), 944–948. doi:10.1038/35082064

566 Burnham, K., & Anderson, D. (2002). *Model selection and multimodel inference* (2nd ed.).
567 New York: Springer.

568 Burton, R. S., & Barreto, F. S. (2012). A disproportionate role for mtDNA in Dobzhansky-
569 Muller incompatibilities? *Molecular Ecology*, *21*(20), 4942–4957.
570 doi:10.1111/mec.12006

571 Byrne, M. (2008). Evidence for multiple refugia at different time scales during Pleistocene
572 climatic oscillations in southern Australia inferred from phylogeography. *Quaternary*
573 *Science Reviews*, *27*, 2576–2585. doi:10.1016/j.quascirev.2008.08.032

574 Clement, M., Posada, D., & Crandall, K. A. (2000). TCS: a computer program to estimate
575 gene genealogies. *Molecular Ecology*, *9*(10), 1657–1659. doi:10.1046/j.1365-
576 294x.2000.01020.x

577 Corl, A., Davis, A. R., Kuchta, S. R., & Sinervo, B. (2010). Selective loss of polymorphic
578 mating types is associated with rapid phenotypic evolution during morphic speciation.
579 *Proceedings of the National Academy of Sciences*, *107*(9), 4254–4259.
580 doi:10.1073/pnas.0909480107

581 Coyne, J. A., & Orr, H. A. (2004). *Speciation*. *Sinauer Associates*. Sunderland,
582 Massachusetts: Sinauer Associates.

583 Derryberry, E. P., Derryberry, G. E., Maley, J. M., & Brumfield, R. T. (2014). HZAR: hybrid
584 zone analysis using an R software package. *Molecular Ecology Resources*, *14*(3), 652–
585 663. doi:10.1111/1755-0998.12209

586 Dobzhansky, T. (1937). *Genetics the Origin and of Species*. *Genetics and the origin of*
587 *species*. New York: Columbia University Press.

588 Earl, D. A., & VonHoldt, B. M. (2012). STRUCTURE HARVESTER: a website and program
589 for visualizing STRUCTURE output and implementing the Evanno mothod.
590 *Conservation Genetics Resources*, *4*(2), 359–360. doi:10.1007/s12686-011-9548-7

591 Ellison, C. K., & Burton, R. S. (2008). Interpopulation hybrid breakdown maps to the

592 mitochondrial genome. *Evolution*, *62*(3), 631–638. doi:10.1111/j.1558-
593 5646.2007.00305.x

594 Fishman, L., & Willis, J. H. (2006). A cytonuclear incompatibility causes anther sterility in
595 *Mimulus* hybrids. *Evolution*, *60*(7), 1372–1381. doi:10.1554/05-708.1

596 Forsman, A., Ahnesjö, J., Caesar, S., & Karlsson, M. (2008). A model of ecological and
597 evolutionary consequences of color polymorphism. *Ecology*, *89*(1), 34–40.
598 doi:10.1890/07-0572.1

599 Forstner, M. R., Davis, S. K., & Arèvalo, E. (1995). Support for the hypothesis of anguimorph
600 ancestry for the suborder Serpentes from phylogenetic analysis of mitochondrial DNA
601 sequences. *Molecular Phylogenetics and Evolution*, *4*(1), 93–102.
602 doi:10.1006/mpev.1995.1010

603 Gay, L., Crochet, P. A., Bell, D. A., & Lenormand, T. (2008). Comparing clines on molecular
604 and phenotypic traits in hybrid zones: A window on tension zone models. *Evolution*,
605 *62*(11), 2789–2806. doi:10.1111/j.1558-5646.2008.00491.x

606 Georges, A., Li, Q., Lian, J., O'Meally, D., Deakin, J., Wang, Z., … Zhang, G. (2015). High-
607 coverage sequencing and annotated assembly of the genome of the Australian dragon
608 lizard *Pogona vitticeps*. *GigaScience*, *4*(1), 45. doi:10.1186/s13742-015-0085-2

609 Gibbons, J. R. H. (1977). *Comparative ecology and behaviour of lizards of the* Amphibolurus
610 decresii *species complex*. PhD dissertation. The University of Adelaide.

611 Gibbons, J. R. H. (1979). The hind leg pushup display of the *Amphibolurus decresii* species
612 complex (Lacertilia: Agamidae). *Copeia*, *1*, 29–40. doi:10.2307/1443725

613 Gray, S. M., & McKinnon, J. S. (2007). Linking color polymorphism maintenance and
614 speciation. *Trends in Ecology & Evolution*, *22*(2), 71–79. doi:10.1016/j.tree.2006.10.005

615 Gruber, B., Unmack, P. J., Berry, O. F., & Georges, A. (2018). dartR: An R package to
616 facilitate analysis of SNP data generated from reduced representation genome
617 sequencing. *Molecular Ecology Resources*, *18*, 691–699. doi:10.1111/1755-0998.12745

618 Hacking, J. D., Stuart-Fox, D., Godfrey, S. S., & Gardner, M. G. (2018). Specific MHC class
619 I supertype associated with parasite infection and color morph in a wild lizard
620 population. *Ecology and Evolution*, *8*(19), 9920–9933. doi:10.1002/ece3.4479

621 Hill, G. E. (2015). Mitonuclear ecology. *Molecular Biology and Evolution*, *32*(8), 1917–1927.
622 doi:10.1093/molbev/msv104

623 Houston, T. F. (1974). Revision of the *Amphibolurus decresii* complex (Lacertilia: Agamidae)
624 of South Australia. *Transactions of The Royal Society of South Australia*, *98*(2), 49–60.
625 doi:10.1126/science.97.2526.482-a

626 Hugall, A. F., & Stuart-Fox, D. (2012). Accelerated speciation in colour-polymorphic birds.
627 *Nature*, *485*, 631–634. doi:10.1038/nature11050

628 Huxley, J. (1955). Morphism in birds. *Acta International Congress Ornithology XI*, 309–328.

629 Jakobsson, M., & Rosenberg, N. A. (2007). CLUMPP: A cluster matching and permutation
630 program for dealing with label switching and multimodality in analysis of population

631 structure. *Bioinformatics*, *23*(14), 1801–1806. doi:10.1093/bioinformatics/btm233

632 Jiggins, C. D., Naisbit, R. E., Coe, R. L., & Mallet, J. (2001). Reproductive isolation caused
633 by colour pattern mimicry. *Nature*, *411*(6835), 302–305. doi:10.1038/35077075

634 Jombart, T., & Ahmed, I. (2011). adegenet 1.3-1: New tools for the analysis of genome-wide
635 SNP data. *Bioinformatics*, *27*(21), 3070–3071. doi:10.1093/bioinformatics/btr521

636 Kalinowski, S. T., Taper, M. L., & Marshall, T. C. (2007). Revising how the computer
637 program CERVUS accommodates genotyping error increases success in paternity
638 assignment. *Molecular Ecology*, *16*(5), 1099–1106. doi:10.1111/j.1365-
639 294X.2007.03089.x

640 Kearse, M., Moir, R., Wilson, A., Stones-havas, S., Sturrock, S., Buxton, S., … Drummond,
641 A. (2012). Geneious Basic: An integrated and extendable desktop software platform for
642 the organization and analysis of sequence data. *Bioinformatics*, *28*(12), 1647–1649.
643 doi:10.1093/bioinformatics/bts199

644 Kilian, A., Wenzl, P., Huttner, E., Carling, J., Xia, L., Caig, V., … Uszynski, G. (2012).
645 Diversity Arrays Technology: A Generic Genome Profiling Technology on Open
646 Platforms. In F. Pompanon & A. Bonin (Eds.), *Data Production and Analysis in*
647 *Population Genomics. Methods in Molecular Biology (Methods and Protocols)* (Vol.
648 888, pp. 67–89). Totowa, NJ: Humana Press. doi:10.1007/978-1-61779-870-2

649 Küpper, C., Stocks, M., Risse, J. E., Dos Remedios, N., Farrell, L. L., McRae, S. B., …
650 Burke, T. (2016). A supergene determines highly divergent male reproductive morphs in
651 the ruff. *Nature Genetics*, *48*(1), 79–83. doi:10.1038/ng.3443

652 Lank, D. B., Smith, C. M., Hanotte, O., Burke, T., & Cooke, F. (1995). Genetic
653 polymorphism for alternative mating behaviour in lekking male ruff *Philomachus*
654 *pugnax*. *Nature*, *378*(2), 59–62. doi:10.1038/378059a0

655 Lê, S., Josse, J., & Husson, F. (2008). FactoMineR: An R Package for Multivariate Analysis.
656 *Journal of Statistical Software*, *25*(1), 1–18. doi:10.1016/j.envint.2008.06.007

657 Lukacs, P. M., Burnham, K. P., & Anderson, D. R. (2010). Model selection bias and
658 Freedman's paradox. *Annals of the Institute of Statistical Mathematics*, *62*(1), 117–125.
659 doi:10.1007/s10463-009-0234-4

660 Maia, R., Gruson, H., Endler, J. A., & White, T. E. (2019). PAVO 2: New tools for the
661 spectral and spatial analysis of colour in R. *Methods in Ecology and Evolution*, *10*(7),
662 1097–1107. doi:10.1111/2041-210X.13174

663 Marshall, T. C., Slate, J., Kruuk, L. E. B., & Pemberton, J. M. (1998). Statistical confidence
664 for likelihood-based paternity inference in natural populations. *Molecular Ecology*, *7*,
665 639–655.

666 Mavárez, J., Salazar, C. A., Bermingham, E., Salcedo, C., Jiggins, C. D., & Linares, M.
667 (2006). Speciation by hybridization in *Heliconius* butterflies. *Nature*, *441*(7095), 868–
668 871. doi:10.1038/nature04738

669 Maynard-Smith, J. (1996). Sympatric speciation. *The American Naturalist*, *916*, 637–650.

670 McKinnon, J. S., & Pierotti, M. E. R. (2010). Colour polymorphism and correlated characters:

671 genetic mechanisms and evolution. *Molecular Ecology*, *19*(23), 5101–5125.
672 doi:10.1111/j.1365-294X.2010.04846.x

673 McLean, C. A., Lutz, A., Rankin, K. J., Stuart-Fox, D., & Moussalli, A. (2017). Revealing the
674 biochemical and genetic basis of color variation in a polymorphic lizard. *Molecular*
675 *Biology and Evolution*, *34*(8), 1924–1935. doi:10.1093/molbev/msx136

676 McLean, C. A., Moussalli, A., & Stuart-Fox, D. (2014). Local adaptation and divergence in
677 colour signal conspicuousness between monomorphic and polymorphic lineages in a
678 lizard. *Journal of Evolutionary Biology*, *27*(12), 2654–2664. doi:10.1111/jeb.12521

679 McLean, C. A., & Stuart-Fox, D. (2014). Geographic variation in animal colour
680 polymorphisms and its role in speciation. *Biological Reviews*, *89*(4), 860–873.
681 doi:10.1111/brv.12083

682 McLean, C. A., Stuart-Fox, D., & Moussalli, A. (2014). Phylogeographic structure,
683 demographic history and morph composition in a colour polymorphic lizard. *Journal of*
684 *Evolutionary Biology*, *27*(10), 2123–2137. doi:10.1111/jeb.12464

685 McLean, C. A., Moussalli, A., Sass, S., & Stuart-Fox, D. (2013). Taxonomic assessment of
686 the *Ctenophorus decresii* (Reptilia: Agamidae) complex reveals a new species of dragon
687 lizard from western New South Wales. *Records of the Australian Museum*, *65*, 51–63.

688 McLean, C. A., Stuart-Fox, D., & Moussalli, A. (2015). Environment, but not genetic
689 divergence, influences geographic variation in colour morph frequencies in a lizard.
690 *BMC Evolutionary Biology*, *15*(1), 156. doi:10.1186/s12862-015-0442-x

691 Meiklejohn, C. D., Holmbeck, M. A., Siddiq, M. A., Abt, D. N., Rand, D. M., & Montooth,
692 K. L. (2013). An incompatibility between a mitochondrial tRNA and its nuclear-encoded
693 tRNA synthetase compromises development and fitness in *Drosophila*. *PLoS Genetics*,
694 *9*(1), e1003238. doi:10.1371/journal.pgen.1003238

695 Melville, J., Haines, M. L., Boysen, K., Hodkinson, L., Kilian, A., Smith Date, K. L., …
696 Parris, K. M. (2017). Identifying hybridization and admixture using SNPs: application of
697 the DArTseq platform in phylogeographic research on vertebrates. *Royal Society Open*
698 *Science*, *4*, 161061. doi:10.1098/rsos.161061

699 Muller, H. J. (1942). Isolating mechanisms, evolution, and temperature. *Biol Symp*, *6*, 71–125.

700 Niehuis, O., Judson, A. K., & Gadau, J. (2008). Cytonuclear genic incompatibilities cause
701 increased mortality in male F2 hybrids of *Nasonia giraulti* and *N. vitripennis*. *Genetics*,
702 *178*(1), 413–426. doi:10.1534/genetics.107.080523

703 O'Neill, E. M., & Beard, K. H. (2010). Genetic basis of a color pattern polymorphism in the
704 coqui frog *Eleutherodactylus coqui*. *Journal of Heredity*, *101*(6), 703–709.
705 doi:10.1093/jhered/esq082

706 Osborne, L., Umbers, K. D. L., Backwell, P. R. Y., & Keogh, J. S. (2012). Male tawny
707 dragons use throat patterns to recognize rivals. *Naturwissenschaften*, *99*(10), 869–872.
708 doi:10.1007/s00114-012-0968-3

709 Pardo-Diaz, C., Salazar, C., Baxter, S. W., Merot, C., Figueiredo-Ready, W., Joron, M., …
710 Jiggins, C. D. (2012). Adaptive introgression across species boundaries in *Heliconius*
711 butterflies. *PLoS Genetics*, *8*(6), e1002752. doi:10.1371/journal.pgen.1002752

712 Pritchard, J. K., Stephens, M., & Donnelly, P. (2000). Inference of population structure using
713 multilocus genotype data. *Genetics*, *155*(2), 945–959. doi:10.1111/j.1471-
714 8286.2007.01758.x

715 Pryke, S. R., & Griffith, S. C. (2009). Postzygotic genetic incompatibility between sympatric
716 color morphs. *Evolution*, *63*(3), 793–798. doi:10.1111/j.1558-5646.2008.00584.x

717 Ramos, J. A., & Peters, R. A. (2016). Dragon wars: Movement-based signalling by Australian
718 agamid lizards in relation to species ecology. *Austral Ecology*, *41*, 302–315.
719 doi:10.1111/aec.12312

720 Rankin, K. J., McLean, C. A., Kemp, D. J., & Stuart-Fox, D. (2016). The genetic basis of
721 discrete and quantitative colour variation in the polymorphic lizard, *Ctenophorus*
722 *decresii*. *BMC Evolutionary Biology*, *16*(1), 1–14. doi:10.1186/s12862-016-0757-2

723 Rankin, K. J., & Stuart-Fox, D. (2015). Testosterone-induced expression of male colour
724 morphs in females of the polymorphic tawny dragon lizard, *Ctenophorus decresii*. *PLOS*
725 *ONE*, *10*(10), e0140458. doi:10.1371/journal.pone.0140458

726 Sætre, G. P., Moum, T., Bureš, S., Král, M., Adamjan, M., Moreno, J., … Moreno, J. (1997).
727 A sexually selected character displacement in flycatchers reinforces premating isolation.
728 *Nature*, *387*(June), 589–592. doi:10.1038/42451

729 Schwartz, T. S., Warner, D. A., Beheregaray, L. B., Olsson, M., & Note, P. (2007).
730 Microsatellite loci for Australian agamid lizards. *Molecular Ecology Notes*, *7*(3), 528–
731 531. doi:10.1111/j.1471-8286.2006.01644.x

732 Scott, I. A. W. W., & Keogh, J. S. (2000). Conservation genetics of the endangered grassland
733 earless dragon *Tympanocryptis pinguicolla* (Reptilia: Agamidae) in Southeastern
734 Australia. *Conservation Genetics*, *1*(4), 357–363. doi:10.1023/A:1011542717349

735 Seehausen, O., Terai, Y., Magalhaes, I. S., Carleton, K. L., Mrosso, H. D. J., Miyagi, R., …
736 Okada, N. (2008). Speciation through sensory drive in cichlid fish. *Nature*, *455*(7213),
737 620-U23. doi:10.1038/nature07285

738 Sinervo, B., & Svensson, E. (2002). Correlational selection and the evolution of genomic
739 architecture. *Heredity*, *89*(5), 329–338. doi:10.1038/sj.hdy.6800148

740 Sinervo, B., & Lively, C. M. (1996). The rock-paper-scissors game and the evolution of
741 alternative male strategies. *Nature*, *380*(6571), 240–243.

742 Sinervo, B., Bleay, C., Adamopoulou, C., Inervo, B. A. S., & Leay, C. O. B. (2001). Social
743 causes of correlational selection and the resolution of a heritable throat color
744 polymorphism in a lizard. *Evolution*, *55*(10), 2040–2052. doi:10.1554/0014-
745 3820(2001)055

746 Smith, K. R., Cadena, V., Endler, J. A., Kearney, M. R., Porter, W. P., & Stuart-Fox, D.
747 (2016). Color change for thermoregulation versus camouflage in free-ranging lizards.
748 *American Naturalist*, *188*(6), 668–678. doi:10.1086/688765

749 Stein, A. C., & Uy, J. A. C. (2006). Unidirectional introgression of a sexually selected trait
750 across an avian hybrid zone: a role for female choice? *Evolution*, *60*(7), 1476–1485.
751 doi:10.1111/j.0014-3820.2006.tb01226.x

Stevens, M., Párraga, C. A., Cuthill, I. C., Partridge, J. C., & Troscianko, T. S. (2007). Using digital photography to study animal coloration. *Biological Journal of the Linnean Society*, *90*, 211–237. doi:10.1111/j.1095-8312.2007.00725.x

Stuart-Fox, D., & Johnston, G. R. (2005). Experience overrides colour in lizard contests. *Behaviour*, *142*, 329–350. doi:10.1163/1568539053778265

Symonds, M. R. E., & Moussalli, A. (2011). A brief guide to model selection, multimodel inference and model averaging in behavioural ecology using Akaike's information criterion. *Behavioral Ecology and Sociobiology*, *65*, 13–21. doi:10.1007/s00265-010-1037-6

Szymura, J. M., & Barton, N. H. (1986). Genetic analysis of a hybrid zone between the fire-bellied toads, *Bombina bombina* and *B . variegata*, near Cracow in Southern Poland. *Evolution*, *40*(6), 1141–1159.

Szymura, J. M., & Barton, N. H. (1991). The genetic structure of the hybrid zone between the fire-bellied toads *Bombina bombina* and *B. variegata*: comparisons between transects and between loci. *Evolution*, *45*(2), 237–261. doi:10.1111/j.1558-5646.1991.tb04400.x

Teasdale, L. C., Stevens, M., & Stuart-Fox, D. (2013). Discrete colour polymorphism in the tawny dragon lizard (*Ctenophorus decresii*) and differences in signal conspicuousness among morphs. *Journal of Evolutionary Biology*, *26*(5), 1035–1046. doi:10.1111/jeb.12115

Vähä, J. P., & Primmer, C. R. (2006). Efficiency of model-based Bayesian methods for detecting hybrid individuals under different hybridization scenarios and with different numbers of loci. *Molecular Ecology*, *15*(1), 63–72. doi:10.1111/j.1365-294X.2005.02773.x

Venables, W. N., & Ripley, B. D. (2002). *Modern Applied Statistics with S* (Fourth). New York: Springer. Retrieved from http://www.stats.ox.ac.uk/pub/MASS4

Wellenreuther, M., Svensson, E. I., & Hansson, B. (2014). Sexual selection and genetic colour polymorphisms in animals. *Molecular Ecology*, *23*(22), 5398–5414. doi:10.1111/mec.12935

West-Eberhard, M. J. (1986). Alternative adaptations, speciation, and phylogeny (A Review). *Proceedings of the National Academy of Sciences*, *83*, 1388–1392. doi:10.1073/pnas.83.5.1388

While, G. M., Michaelides, S., Heathcote, R. J. P., Macgregor, H. E. A., Zajac, N., Beninde, J., … Uller, T. (2015). Sexual selection drives asymmetric introgression in wall lizards. *Ecology Letters*, *18*(12), 1366–1375. doi:10.1111/ele.12531

Yewers, M. S. C., Jessop, T. S., & Stuart-Fox, D. (2017). Endocrine differences among colour morphs in a lizard with alternative behavioural strategies. *Hormones and Behavior*, *93*, 118–127. doi:10.1016/j.yhbeh.2017.05.001

Yewers, M. S. C., Pryke, S. R., & Stuart-Fox, D. (2016). Behavioural differences across contexts may indicate morph-specific strategies in the lizard *Ctenophorus decresii*. *Animal Behaviour*, *111*, 329–339. doi:10.1016/j.anbehav.2015.10.029

793 **Tables**

794

795 **Table 1.** Populations sampled across the species range [Northern Flinders Ranges (NFR),
796 Southern Flinders Ranges (SFR), Olary Ranges (OR), Contact Zone (CZ), Mainland South
797 (MS), and Kangaroo Island (KI)] with details of sample size for the SNP dataset (*N*), expected
798 and observed heterozygosity (H_{exp}, H_{obs}), inbreeding coefficient (F), allele number (AN), and
799 allelic richness (AR).

800

Population	*N* (♂ / ♀ / NA)	H_{exp}	H_{obs}	F	AN	AR
NFR	7 (2 / 0 / 5)	0.064	0.055	0.177	1629	0.222
SFR	41 (31 / 8 / 2)	0.076	0.070	0.129	2091	0.569
OR	60 (45 / 7 / 8)	0.072	0.060	0.177	2138	0.604
CZ	82 (69 / 13 / 0)	0.084	0.079	0.095	2134	0.601
MS	33 (26 / 4 / 3)	0.051	0.043	0.175	1714	0.286
KI	7 (6 / 1 / 0)	0.023	0.019	0.165	1429	0.072
Total	230					

801 †Sex was unknown for a portion of loaned museum tissue samples.

802

803 **Table 2.** Model-averaged estimates for cline centre and width based on the AIC 95%
804 confidence set models, with *N* representing the number of models within the AIC confident
805 set. Cline centre is the distance (km) from the southern-most sampling site and width (*w*) is
806 1/slope at the centre. Two log-likelihood unit support limits are shown as 'low' and 'high'.
807 See Table S6 for full details of cline models.

808

Trait		*N*	Centre	(low – high)	Width	(low – high)
Hybrid Index (H_{Index})		10	28.41	(22.37 – 33.00)	29.77	(15.05 – 55.84)
mtDNA		7	27.78	(14.59 – 28.17)	0.64	(0.08 – 21.85)
Dorsolateral Phenotype (D_{PC1})		2	23.02	(16.33 – 27.61)	13.97	(0.82 – 29.02)
Throat Phenotype	QC_{UVS}	4	15.90	(14.25 – 20.48)	8.48	(0.74 – 17.27)
	T_{PC1}	2	15.38	(15.06 – 16.61)	3.22	(2.43 – 7.94)

809

Figures

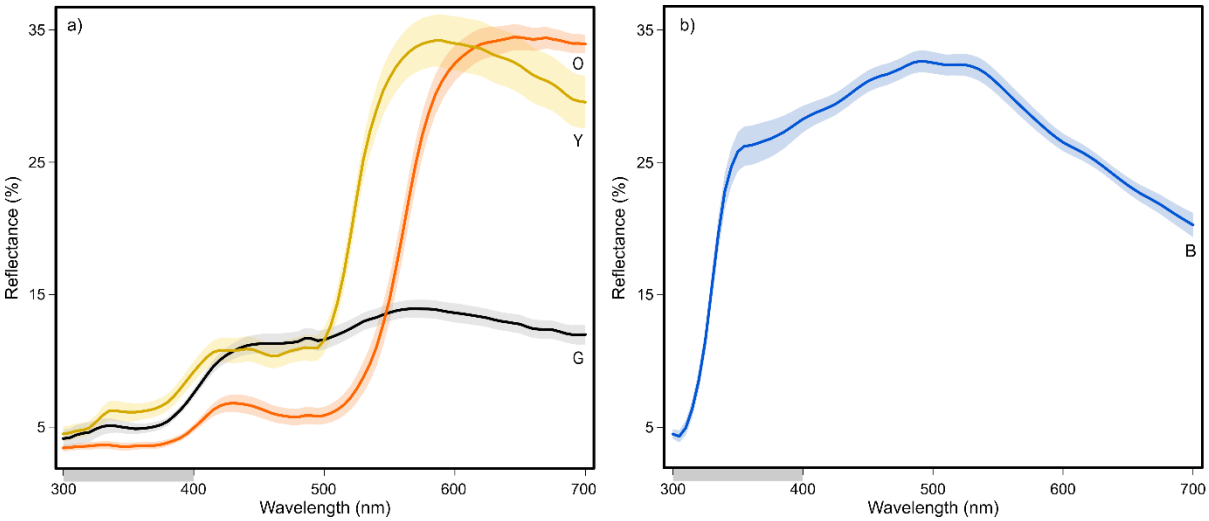

Figure 1. Average spectral reflectances of male throat colours found in *C. decresii*. (a) Northern lineage throat colours: orange (O), yellow (Y), grey (G). (b) Southern lineage ultra-violet blue (B) throat colour. Standard error shown as shaded region (N = 10 for each colour). Ultraviolet wavelengths are shown with a grey bar on the *x*-axis.

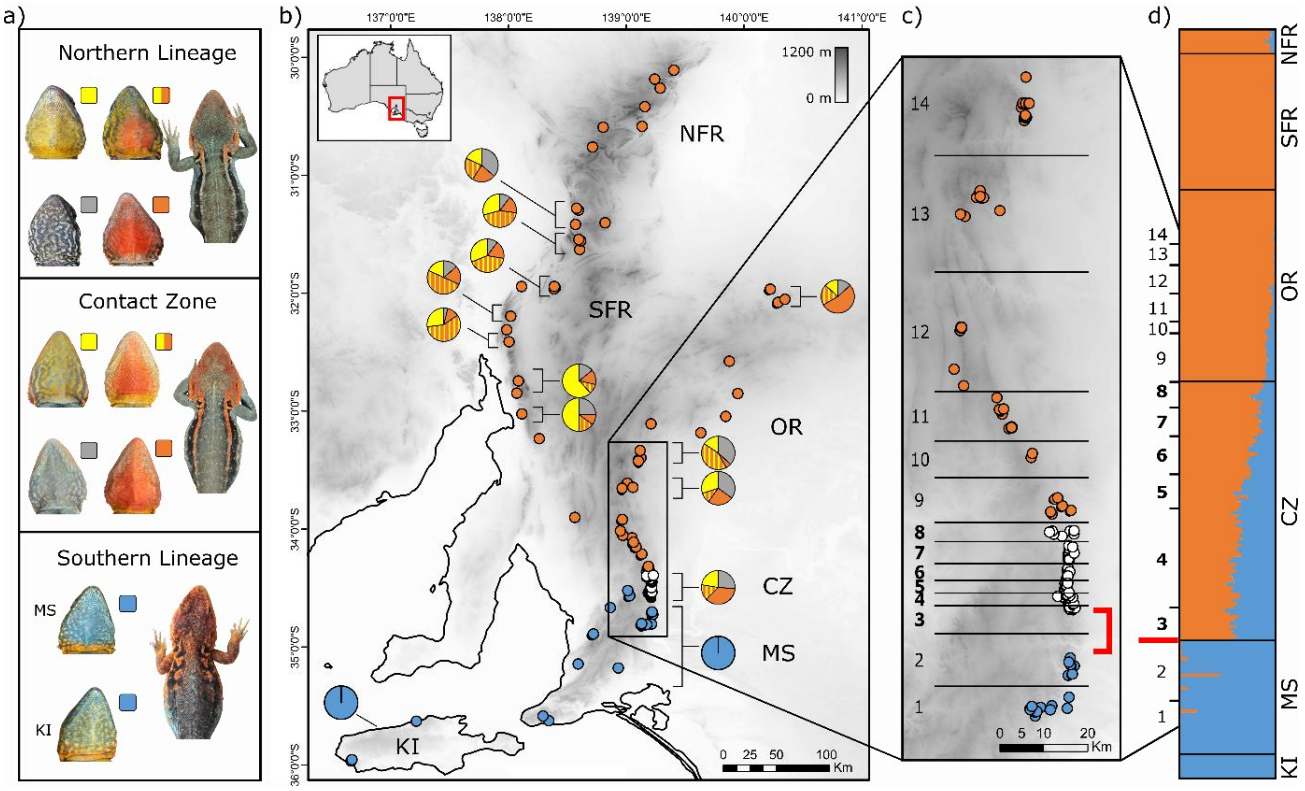

Figure 2. Geographic variation in throat colour morphs and genetic structure between lineages of *C. decresii*. (a) Representative throats (North: yellow, orange-yellow, grey and orange; South: blue) and dorsolateral phenotypes found in each lineage and the contact zone. (b) Map showing sampling localities of individuals used in genetic analyses [Northern Flinders Ranges (NFR), Southern Flinders Ranges (SFR), Olary Ranges (OR), Mainland South (MS), and Kangaroo Island (KI)] and relative frequencies of male throat colour morphs within populations. Proportions for the Southern Flinders Ranges and northernmost population in the Olary Ranges are adapted from McLean, Stuart-Fox, & Moussalli, 2015. Throat colour morph data are not available for the Northern Flinders Ranges. Elevation in meters is represented by grey shading on the scale bar. (c) An enlarged map section showing sites across the contact zone transect used for geographic cline analyses; (d) Results of a Bayesian analysis of ancestry in the program STRUCTURE (K = 2). Each horizontal bar represents an individual and individuals are ordered by latitude and population. The proportion of blue and orange represents the proportion of southern and northern ancestry in each individual. A density trough between sites 2 and 3, where surveys did not recover any individuals, is indicated in red in panels B and C.

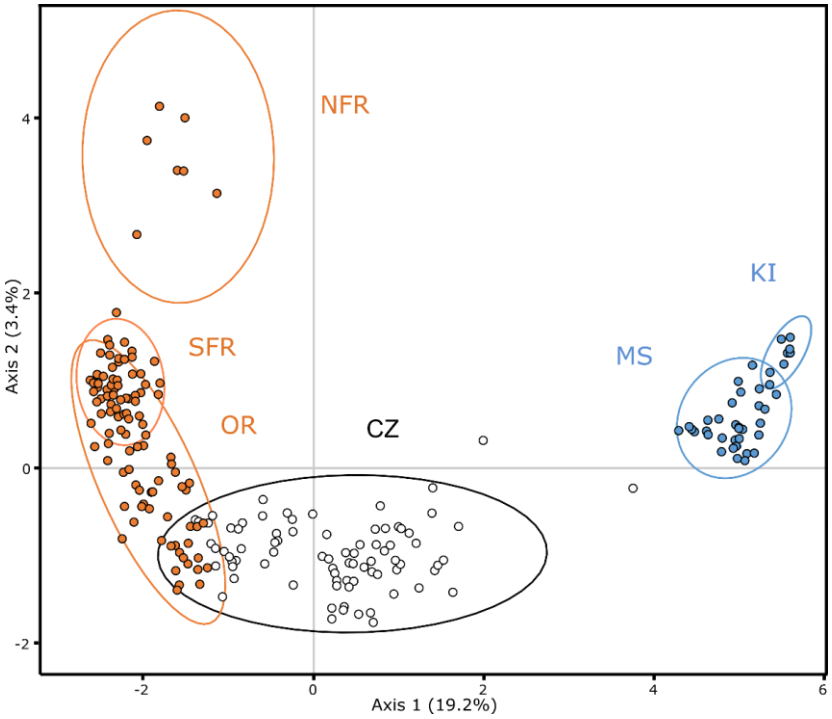

837

838

839 **Figure 3.** Two-dimensional principal coordinate plot (PCoA) constructed from the full SNP
840 data set (1,333 loci) showing pairwise genetic distances between individuals. 95% confidence
841 ellipses of each population are shown [Northern Flinders Ranges (NFR), Southern Flinders
842 Ranges (SFR), Olary Ranges (OR), Contact Zone (CZ), Mainland South (MS), and Kangaroo
843 Island (KI)]. Two outlying admixed individuals (from the 95% confidence ellipse) were those
844 found in the southern geographic range (MS).

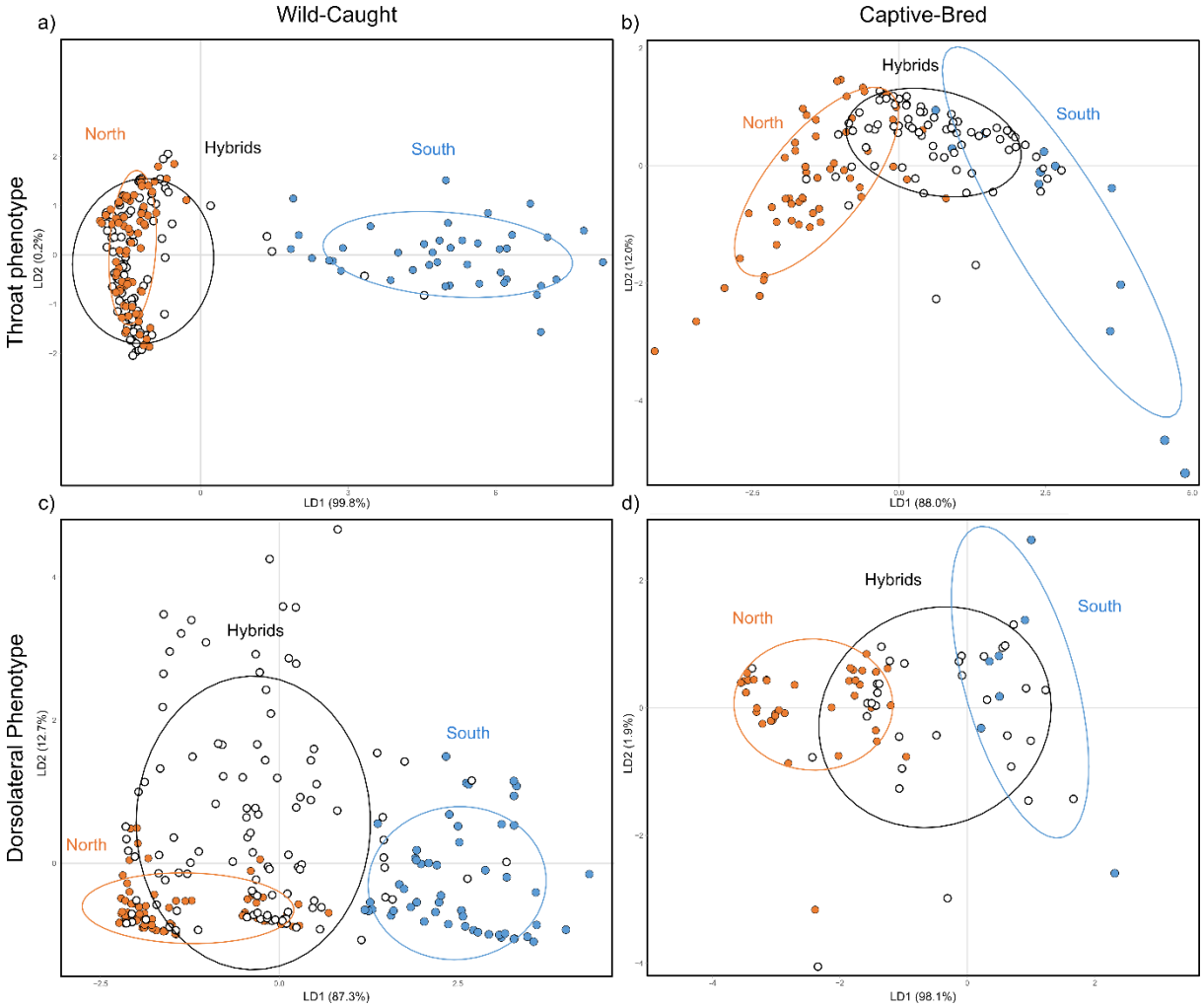

845

846

847 **Figure 4**. Biplots of linear discriminant analyses on (a, b) throat and (c, d) dorsolateral
848 phenotype variables for (a, c) wild-caught individuals along the contact zone transect and (b,
849 d) captive-bred pure and F1 hybrid offspring. 95% confidence ellipses are shown.

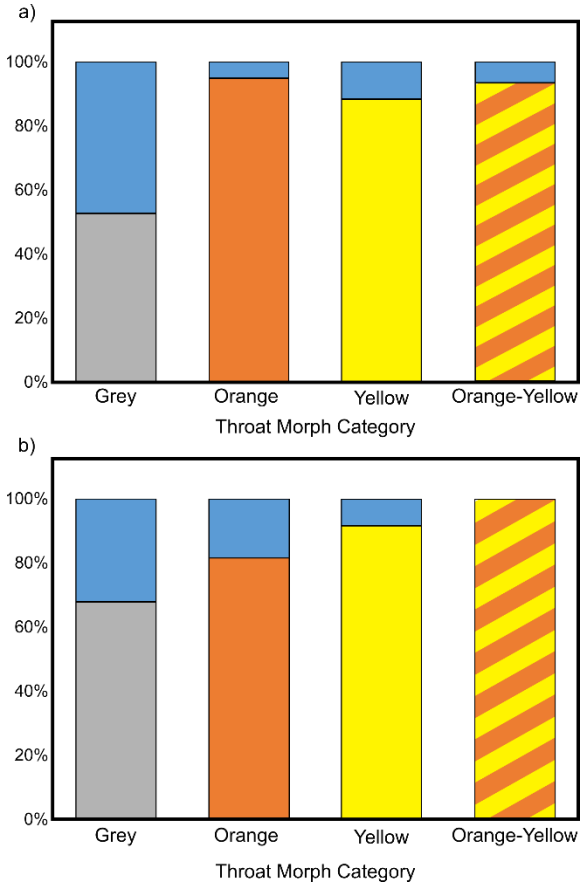

850

851

852 **Figure 5.** Percentage of individuals in each throat morph category which exhibit a degree of
853 blue coloration on the throat for (a) wild-caught male hybrids and (b) captive-bred F1 hybrids
854 (both sexes).

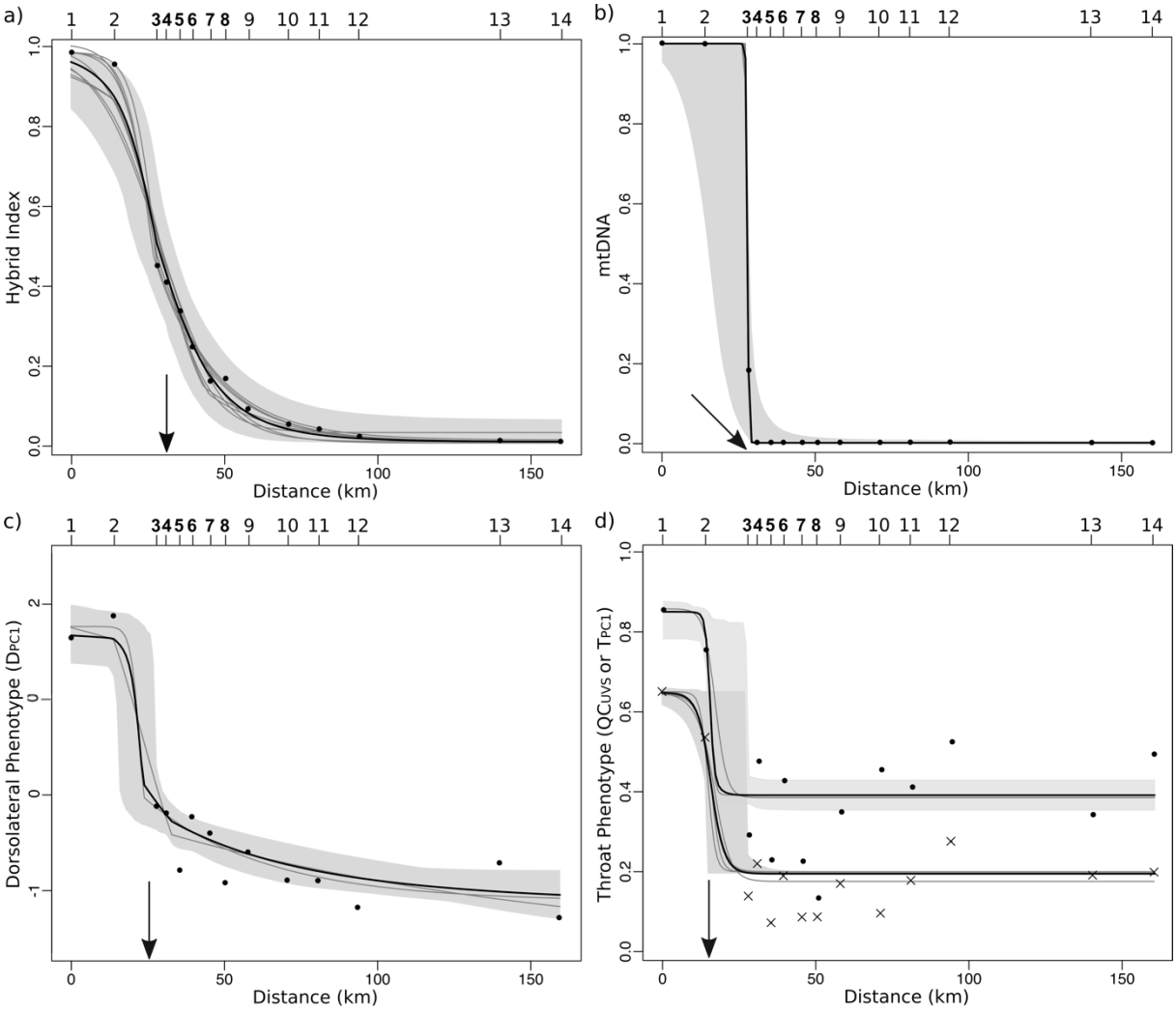

Figure 6. AICc model-averaged geographic clines (black) and credible regions, clines comprising the 95% confidence set of models (grey), and observed frequencies at each site for (a) the hybrid index estimated from 1333 loci (N = 154), (b) mtDNA haplotype frequencies (N = 74), (c) dorsolateral phenotype (D_{PC1}; N = 233), and (d) throat phenotype clines (N = 204 for both): quantum catch of UV receptor (QC_{UVS}; lower cline, frequencies shown with '×' symbols) and throat colouration (T_{PC1}; upper cline). Numbers along the top refer to sampling sites (see Table S2 for sample sizes at each site), bolded sites (3 – 8) comprise the contact zone. Transect distance is the cumulative distance from the southern-most population with increasing distance northwards. Arrows indicate cline centres; throat phenotype clines have essentially the same centres and are indicated with one arrow.

Supplemental Information

Table S1. Details of all individuals used in the study, including if the individual was sequenced (SNPs and/or mitochondrial ND4 gene), had dorsal/ventral photos and spectral reflectance measurements, and the sex (M = male, F = female). Population [Southern: Kangaroo Island (KI), Mainland South (MS); Northern: Northern Flinders Ranges (NFR), Southern Flinders Ranges (SFR), Olary Ranges (OR); and Contact Zone (CZ)], year, and cline site (if applicable) are shown.

ID	SNPs	ND4	Photos	Specs	Sex	Pop	Year	Cline Site	Latitude	Longitude
KI206	Y	N	N	N	M	KI	2010	NA	-35.965	136.653
KI208	Y	N	N	N	M	KI	2011	NA	-35.965	136.653
KI194	Y	N	N	N	F	KI	2010	NA	-35.964	136.653
KI179	Y	N	N	N	M	KI	2010	NA	-35.963	136.654
KI193	Y	N	N	N	M	KI	2010	NA	-35.963	136.654
KI181	Y	N	N	N	M	KI	2010	NA	-35.960	136.655
KI215	Y	N	N	N	M	KI	2011	NA	-35.621	137.210
R45184	Y	N	N	N	NA	MS	1994	NA	-35.642	138.329
R49234	Y	N	N	N	NA	MS	1996	NA	-35.601	138.279
R53785	Y	N	N	N	F	MS	2000	NA	-35.194	138.919
R55041	Y	N	N	N	F	MS	2000	NA	-35.160	138.578
M232	Y	N	N	N	M	MS	2011	NA	-34.908	138.707
M235	Y	N	N	N	M	MS	2011	NA	-34.906	138.702
M248	Y	N	N	N	M	MS	2011	NA	-34.906	138.707
R42978	Y	N	N	N	NA	MS	1993	NA	-34.683	138.850
631	Y	N	N	N	M	MS	2012	NA	-34.582	139.015
KS630	Y	N	N	N	M	MS	2012	NA	-34.582	139.015
KS631	Y	N	N	N	M	MS	2012	NA	-34.582	139.015
KS632	Y	N	N	N	M	MS	2012	NA	-34.582	139.015
KS634	Y	N	N	N	F	MS	2012	NA	-34.581	139.015
R27416	N	Y	N	N	NA	MS	2012	1	-34.842	139.133
638	N	Y	N	N	F	MS	2012	1	-34.831	139.130
639	N	Y	N	N	F	MS	2012	1	-34.494	139.201
640	N	Y	N	N	F	MS	2012	1	-34.830	139.129
641	N	Y	N	N	M	MS	2012	1	-34.494	139.201
642	N	Y	N	N	F	MS	2012	1	-34.833	139.128
PB1	Y	N	Y	N	M	MS	2013	1	-34.834	139.128
S42	Y	N	Y	Y	M	MS	2016	1	-34.830	139.129

S32	N	N	Y	Y	M	MS	2015	1	-34.830	139.128
S44	N	N	Y	Y	M	MS	2016	1	-34.829	139.129
S31	Y	Y	Y	Y	M	MS	2015	1	-34.829	139.130
S39	N	N	Y	Y	M	MS	2015	1	-34.829	139.129
S47	Y	Y	Y	Y	M	MS	2016	1	-34.828	139.124
S30	N	N	Y	Y	M	MS	2015	1	-34.826	139.129
S40	N	N	Y	Y	M	MS	2015	1	-34.826	139.160
S33	N	N	Y	Y	M	MS	2015	1	-34.822	139.162
S29	Y	N	Y	Y	M	MS	2015	1	-34.822	139.116
S8	Y	Y	N	N	F	MS	2015	1	-34.822	139.116
S27	N	N	Y	Y	M	MS	2015	1	-34.821	139.121
S28	N	N	Y	Y	M	MS	2015	1	-34.821	139.121
PB9	N	N	Y	N	M	MS	2013	1	-34.821	139.160
PB10	N	N	Y	N	M	MS	2013	1	-34.821	139.160
PB4	N	N	Y	N	M	MS	2013	1	-34.820	139.137
PB8	Y	Y	Y	N	M	MS	2013	1	-34.821	139.160
641	N	N	Y	Y	M	MS	2012	1	-34.494	139.201
PB2	N	N	Y	N	M	MS	2013	1	-34.820	139.160
PB3	N	N	Y	N	M	MS	2013	1	-34.820	139.132
PB5	N	N	Y	N	M	MS	2013	1	-34.819	139.162
S21	Y	N	Y	Y	M	MS	2015	1	-34.818	139.162
PB6	N	N	Y	N	M	MS	2013	1	-34.818	139.163
S36	N	N	Y	Y	M	MS	2015	1	-34.818	139.163
PB7	N	N	Y	N	M	MS	2013	1	-34.818	139.164
S26	N	N	Y	Y	M	MS	2015	1	-34.817	139.117
710	Y	N	N	N	M	MS	2013	1	-34.817	139.117
S25	Y	N	Y	Y	M	MS	2015	1	-34.817	139.116
S24	N	N	Y	Y	M	MS	2015	1	-34.817	139.164
S35	N	N	Y	Y	M	MS	2015	1	-34.817	139.114
S22	N	N	Y	Y	M	MS	2015	1	-34.817	139.165
S23	N	N	Y	Y	M	MS	2015	1	-34.817	139.165
S37	N	N	Y	Y	M	MS	2015	1	-34.816	139.163
S38	N	N	Y	Y	M	MS	2015	1	-33.022	138.000
1142	N	N	Y	Y	M	MS	2017	2	-34.793	139.203
1179	N	N	Y	Y	M	MS	2017	2	-34.742	139.212
1177	Y	N	Y	Y	M	MS	2017	2	-34.742	139.211
1178	N	N	Y	Y	M	MS	2017	2	-34.740	139.211
1145	Y	N	Y	Y	M	MS	2017	2	-34.726	139.214
1146	Y	N	Y	Y	M	MS	2017	2	-34.725	139.214
703	Y	N	Y	N	M	MS	2013	2	-34.725	139.214
1140	N	N	Y	Y	M	MS	2017	2	-34.723	139.216
1143	N	N	Y	Y	M	MS	2017	2	-34.723	139.214
1141	Y	N	Y	Y	M	MS	2017	2	-34.723	139.215

1144	Y	N	Y	Y	M	MS	2017	2	-34.723	139.215
1171	N	N	Y	Y	M	MS	2017	2	-34.721	139.215
1164	N	N	Y	Y	M	MS	2017	2	-34.721	139.215
1167	N	N	Y	Y	M	MS	2017	2	-34.721	139.213
1168	Y	N	Y	Y	M	MS	2017	2	-34.721	139.213
1169	N	N	Y	Y	M	MS	2017	2	-34.721	139.213
1170	N	N	Y	Y	M	MS	2017	2	-34.721	139.213
1166	N	N	Y	Y	M	MS	2017	2	-34.720	139.213
709	Y	Y	N	N	M	MS	2013	2	-34.720	139.207
700	N	N	Y	N	M	MS	2013	2	-34.720	139.214
1165	Y	N	Y	Y	M	MS	2017	2	-34.720	139.214
706	Y	N	N	N	M	MS	2013	2	-34.718	139.206
S1107	Y	N	Y	Y	M	MS	2016	2	-34.701	139.206
1180	N	N	Y	Y	M	CZ	2017	3	-34.591	139.218
H1106	Y	N	Y	Y	M	CZ	2016	3	-34.590	139.218
1186	N	N	Y	Y	M	CZ	2017	3	-34.590	139.209
1185	Y	Y	Y	Y	M	CZ	2017	3	-34.589	139.211
1187	N	N	Y	Y	M	CZ	2017	3	-34.588	139.215
1184	N	N	Y	Y	M	CZ	2017	3	-34.588	139.215
H1104	Y	Y	N	N	F	CZ	2016	3	-34.588	139.218
1182	N	N	Y	Y	M	CZ	2017	3	-34.588	139.217
1183	N	N	Y	Y	M	CZ	2017	3	-34.587	139.216
759	Y	N	Y	N	M	CZ	2013	3	-34.587	139.207
758	N	N	Y	N	M	CZ	2013	3	-34.587	139.206
756	Y	Y	Y	N	M	CZ	2013	3	-34.586	139.206
754	Y	N	N	N	M	CZ	2013	3	-34.586	139.205
1215	N	N	Y	Y	M	CZ	2017	3	-34.585	139.216
1217	N	N	Y	Y	M	CZ	2017	3	-34.585	139.216
1216	N	N	Y	Y	M	CZ	2017	3	-34.585	139.216
H1100	Y	N	Y	Y	M	CZ	2016	3	-34.583	139.215
H1101	Y	N	Y	Y	M	CZ	2016	3	-34.583	139.215
H1102	Y	Y	N	N	F	CZ	2016	3	-34.579	139.215
H1103	Y	Y	N	N	F	CZ	2016	3	-34.577	139.215
H1099	Y	N	Y	Y	M	CZ	2016	3	-34.577	139.203
H1021	Y	N	Y	Y	M	CZ	2015	4	-34.571	139.205
739	Y	N	Y	N	M	CZ	2013	4	-34.564	139.211
738	Y	Y	N	N	F	CZ	2013	4	-34.563	139.208
740	Y	N	Y	N	M	CZ	2013	4	-34.563	139.213
741	Y	Y	N	N	M	CZ	2013	4	-34.563	139.212
737	Y	N	Y	N	M	CZ	2013	4	-34.563	139.207
753	N	N	Y	N	M	CZ	2013	4	-34.561	139.193
716	Y	N	Y	N	M	CZ	2013	4	-34.561	139.202
712	N	N	Y	N	M	CZ	2013	4	-34.561	139.203

713	Y	N	N	N	M	CZ	2013	4	-34.559	139.205
H1020	Y	N	Y	Y	M	CZ	2015	4	-34.558	139.202
H1019	N	N	Y	Y	M	CZ	2015	4	-34.558	139.203
H1009	N	N	Y	Y	M	CZ	2015	4	-34.558	139.177
H1018	N	N	Y	Y	M	CZ	2015	4	-34.557	139.204
715	N	N	Y	N	M	CZ	2013	4	-34.557	139.204
H1017	Y	Y	Y	Y	M	CZ	2015	4	-34.557	139.205
H1051	Y	N	Y	Y	M	CZ	2016	4	-34.557	139.200
H1039	N	N	Y	Y	M	CZ	2015	4	-34.556	139.199
H1007	Y	N	Y	Y	M	CZ	2015	4	-34.556	139.200
H1048	N	N	Y	Y	M	CZ	2015	4	-34.556	139.199
H1008	Y	N	Y	Y	M	CZ	2015	4	-34.556	139.198
H1046	N	N	Y	Y	M	CZ	2015	4	-34.556	139.198
746	N	N	Y	N	M	CZ	2013	4	-34.556	139.199
742	Y	Y	N	N	F	CZ	2013	4	-34.556	139.198
H1049	Y	N	Y	Y	M	CZ	2016	4	-34.556	139.199
743	N	N	Y	N	M	CZ	2013	4	-34.556	139.198
745	N	N	Y	N	M	CZ	2013	4	-34.556	139.197
H1045	N	N	Y	Y	M	CZ	2015	4	-34.556	139.199
H1052	Y	N	N	N	F	CZ	2016	4	-34.556	139.200
H1050	Y	N	Y	Y	M	CZ	2016	4	-34.556	139.200
H1044	N	N	Y	Y	M	CZ	2015	4	-34.556	139.200
H1055	Y	Y	N	N	F	CZ	2016	4	-34.556	139.201
744	N	N	Y	N	M	CZ	2013	4	-34.556	139.202
H1053	Y	Y	Y	Y	M	CZ	2016	4	-34.556	139.200
H1054	Y	N	Y	Y	M	CZ	2016	4	-34.556	139.202
H1056	Y	Y	N	N	F	CZ	2016	4	-34.556	139.202
H1010	N	N	Y	Y	M	CZ	2015	4	-34.556	139.203
H1014	Y	N	Y	Y	M	CZ	2015	4	-34.556	139.203
H1016	Y	Y	Y	Y	M	CZ	2015	4	-34.556	139.202
H1022	Y	Y	Y	Y	M	CZ	2015	4	-34.556	139.201
748	N	N	Y	N	M	CZ	2013	4	-34.556	139.199
H1011	Y	N	Y	Y	M	CZ	2015	4	-34.555	139.203
H1015	N	N	Y	Y	M	CZ	2015	4	-34.555	137.203
H1013	Y	N	Y	Y	M	CZ	2015	4	-34.555	139.203
H1012	Y	N	Y	Y	M	CZ	2015	4	-34.555	139.203
H1023	N	N	Y	Y	M	CZ	2015	4	-34.555	139.202
H1027	Y	Y	Y	Y	M	CZ	2015	4	-34.555	139.206
H1041	N	N	Y	Y	M	CZ	2015	4	-34.555	139.205
750	N	N	Y	N	M	CZ	2013	4	-34.555	139.202
H1042	N	N	Y	Y	M	CZ	2015	4	-34.555	139.204
H1043	N	N	Y	Y	M	CZ	2015	4	-34.555	139.204
H1040	N	N	Y	Y	M	CZ	2015	4	-34.555	139.204

H1029	N	N	Y	Y	M	CZ	2015	4	-34.555	139.204
H1025	Y	N	Y	Y	M	CZ	2015	4	-34.555	139.207
H1026	N	N	Y	Y	M	CZ	2015	4	-34.554	139.207
H1024	N	N	Y	Y	M	CZ	2015	4	-34.554	139.202
H1028	N	N	Y	Y	M	CZ	2015	4	-34.554	139.206
751	N	N	Y	N	M	CZ	2013	4	-34.554	139.202
749	Y	Y	N	N	F	CZ	2013	4	-34.552	139.203
H1086	Y	N	Y	Y	M	CZ	2016	4	-34.551	139.192
H1089	Y	N	Y	Y	M	CZ	2016	5	-34.542	139.197
H1091	Y	Y	Y	Y	M	CZ	2016	5	-34.540	139.202
H1092	Y	Y	Y	Y	M	CZ	2016	5	-34.540	139.202
H1057	Y	N	Y	Y	M	CZ	2016	5	-34.540	139.198
H1059	Y	Y	Y	Y	M	CZ	2016	5	-34.539	139.196
H1090	Y	N	Y	Y	M	CZ	2016	5	-34.539	139.194
636	Y	N	N	N	M	CZ	2012	5	-34.537	138.999
H1097	Y	Y	Y	Y	M	CZ	2016	5	-34.534	139.198
H1060	Y	Y	Y	Y	M	CZ	2016	5	-34.531	139.206
H1093	N	N	Y	Y	M	CZ	2016	5	-34.528	139.197
H1096	Y	N	Y	Y	M	CZ	2016	5	-34.526	139.195
H1098	Y	Y	Y	Y	M	CZ	2016	5	-34.526	139.195
637	N	Y	N	N	F	CZ	2012	6	-34.494	139.201
H1084	Y	N	Y	Y	M	CZ	2016	6	-34.515	139.200
H1075	Y	N	N	N	F	CZ	2016	6	-34.513	139.201
H1076	N	N	Y	Y	M	CZ	2016	6	-34.513	139.201
H1082	Y	Y	Y	Y	M	CZ	2016	6	-34.513	139.200
H1078	Y	N	Y	Y	M	CZ	2016	6	-34.513	139.200
H1079	Y	N	Y	Y	M	CZ	2016	6	-34.508	139.202
H1081	Y	N	Y	Y	M	CZ	2016	6	-34.507	139.202
H1072	N	N	Y	Y	M	CZ	2016	6	-34.503	139.205
H1074	Y	N	Y	Y	M	CZ	2016	6	-34.503	139.205
H1071	Y	Y	Y	Y	M	CZ	2016	6	-34.498	139.201
H1068	Y	N	Y	Y	M	CZ	2016	6	-34.495	139.202
H1069	N	N	Y	Y	M	CZ	2016	6	-34.495	139.202
H1064	Y	N	Y	Y	M	CZ	2016	6	-34.494	139.201
H1065	N	N	Y	Y	M	CZ	2016	6	-34.494	139.202
1218	N	N	Y	Y	M	CZ	2017	6	-34.493	139.202
1220	Y	N	Y	Y	M	CZ	2017	6	-34.492	139.203
H1067	Y	N	Y	Y	M	CZ	2016	6	-34.490	139.203
1222	N	N	Y	Y	M	CZ	2017	6	-34.494	139.200
1221	N	N	Y	Y	M	CZ	2017	6	-34.494	139.201
1223	Y	N	Y	Y	M	CZ	2017	7	34.494	139.201
H1108	Y	N	N	N	M	CZ	2016	7	-34.465	139.203
H1109	Y	N	Y	Y	M	CZ	2016	7	-34.464	139.203

H1111	Y	Y	Y	Y	M	CZ	2016	7	-34.451	139.218
H1110	Y	N	N	N	F	CZ	2016	7	-34.451	139.219
H1113	Y	N	Y	Y	M	CZ	2016	7	-34.449	139.215
H1112	Y	N	Y	Y	M	CZ	2016	7	-34.448	139.209
H1114	Y	N	Y	Y	M	CZ	2016	7	-34.443	39.210
H1115	Y	N	N	N	F	CZ	2016	7	-34.436	139.212
627	N	Y	N	N	M	CZ	2012	8	-34.411	139.159
628	N	Y	N	N	F	CZ	2012	8	-34.411	139.159
629	N	Y	N	N	F	CZ	2012	8	-34.413	139.161
719	Y	Y	N	N	M	CZ	2013	8	-34.421	139.187
721	Y	N	N	N	M	CZ	2013	8	-34.414	139.168
728	Y	N	N	N	M	CZ	2013	8	-34.412	139.164
720	Y	N	N	N	M	CZ	2013	8	-34.411	139.158
H1139	Y	N	Y	Y	M	CZ	2016	8	-34.409	139.210
H1136	Y	N	N	N	F	CZ	2016	8	-34.408	139.215
H1137	Y	N	Y	Y	M	CZ	2016	8	-34.408	139.215
H1117	Y	N	Y	Y	M	OR	2016	9	-34.366	139.164
H1116	Y	Y	Y	Y	M	OR	2016	9	-34.364	139.160
1173	Y	N	Y	Y	M	OR	2017	9	-34.360	139.208
1174	N	N	Y	Y	M	OR	2017	9	-34.360	139.208
1175	Y	N	Y	Y	M	OR	2017	9	-34.358	139.209
1210	N	N	Y	Y	M	OR	2017	9	-34.351	139.190
1224	Y	N	Y	Y	M	OR	2017	9	-34.350	139.188
1225	N	N	Y	Y	M	OR	2017	9	-34.350	139.188
1211	N	N	Y	Y	M	OR	2017	9	-34.350	139.188
1209	N	N	Y	Y	M	OR	2017	9	-34.349	139.189
1208	Y	N	Y	Y	M	OR	2017	9	-34.349	139.188
1212	Y	Y	Y	Y	M	OR	2017	9	-34.348	139.189
1214	Y	N	Y	Y	M	OR	2017	9	-34.348	139.189
1213	Y	N	Y	Y	M	OR	2017	9	-34.348	139.189
1159	N	N	Y	Y	M	OR	2017	9	-34.332	139.173
1176	N	N	Y	Y	M	OR	2017	9	-34.332	139.172
1163	Y	N	Y	Y	M	OR	2017	9	-34.332	139.170
1162	Y	Y	Y	Y	M	OR	2017	9	-34.331	139.173
1160	Y	N	Y	Y	M	OR	2017	9	-34.331	139.174
1161	Y	Y	N	N	F	OR	2017	9	-34.331	139.174
H1121	N	N	Y	Y	M	OR	2016	9	-34.331	139.174
1158	Y	N	Y	Y	M	OR	2017	9	-34.331	139.174
H1122	Y	N	Y	Y	M	OR	2016	9	-34.331	139.173
H1123	Y	Y	Y	Y	M	OR	2016	9	-34.331	139.174
H1124	Y	N	Y	Y	M	OR	2016	10	-34.231	139.118
H1125	Y	Y	Y	Y	M	OR	2016	10	-34.228	139.118
1207	Y	N	Y	Y	M	OR	2017	11	-34.167	139.069

H1133	Y	N	Y	Y	M	OR	2016	11	-34.167	139.069
1206	N	N	Y	Y	M	OR	2017	11	-34.167	139.069
1156	Y	N	Y	Y	M	OR	2017	11	-34.166	139.070
1155	Y	N	Y	Y	M	OR	2017	11	-34.166	139.071
1152	Y	Y	Y	Y	M	OR	2017	11	-34.132	139.048
1148	Y	N	Y	Y	M	OR	2017	11	-34.128	139.048
1154	Y	N	Y	Y	M	OR	2017	11	-34.127	139.048
1149	Y	Y	N	N	F	OR	2017	11	-34.127	139.048
1151	N	N	Y	Y	M	OR	2017	11	-34.127	139.048
H1131	Y	Y	Y	Y	M	OR	2016	11	-34.127	139.049
1153	N	N	Y	Y	M	OR	2017	11	-34.125	139.047
H1135	Y	N	Y	Y	M	OR	2016	12	-34.091	139.035
626	Y	Y	N	N	M	OR	2012	12	-34.070	138.957
R58318	Y	Y	N	N	NA	OR	2003	12	-34.031	138.935
N27	Y	N	Y	Y	M	OR	2015	12	-33.935	138.952
N16	Y	N	Y	Y	M	OR	2015	12	-33.934	138.952
623	Y	N	N	N	M	OR	2012	12	-33.934	138.952
618	Y	Y	N	N	M	OR	2012	12	-33.934	138.952
R26108	Y	N	N	N	NA	OR	1984	12	-33.917	138.550
619	N	Y	N	N	M	OR	2012	12	-33.934	138.952
620	N	Y	N	N	F	OR	2012	12	-33.934	138.952
622	N	Y	N	N	F	OR	2012	12	-33.934	138.952
624	N	Y	N	N	F	OR	2012	12	-	-
625	N	Y	N	N	F	OR	2012	12	-34.070	138.957
N28	N	N	Y	Y	M	OR	2015	12	-33.934	138.953
623	Y	N	N	N	NA	OR	1992	12	-33.934	138.952
R40708	Y	Y	N	N	NA	OR	1992	13	-33.667	138.950
1205	N	N	Y	Y	M	OR	2017	13	-33.662	139.042
1197	N	N	Y	Y	M	OR	2017	13	-33.631	139.004
1195	Y	Y	Y	Y	M	OR	2017	13	-33.631	139.004
1203	N	N	Y	Y	M	OR	2017	13	-33.628	138.996
1194	N	N	Y	Y	M	OR	2017	13	-33.628	139.003
1190	N	Y	Y	Y	M	OR	2017	13	-33.628	139.001
1189	Y	Y	Y	Y	M	OR	2017	13	-33.628	138.999
1193	N	N	Y	Y	M	OR	2017	13	-33.628	139.002
1188	N	N	Y	Y	M	OR	2017	13	-33.627	138.999
1191	Y	N	Y	Y	M	OR	2017	13	-33.627	138.994
1200	Y	Y	Y	Y	M	OR	2017	13	-33.615	138.996
1201	N	N	Y	Y	M	OR	2017	13	-33.615	138.996
1202	N	N	Y	Y	M	OR	2017	13	-33.615	138.996
R41631	N	Y	N	N	M	OR	1992	13	-33.675	138.961
R38012	N	Y	N	N	NA	OR	1991	13	-33.833	139.017
91	N	Y	N	N	M	OR	2010	13	-33.835	139.034

N32	N	N	Y	Y	M	OR	2015	14	-33.444	139.102
N36	Y	N	Y	Y	M	OR	2015	14	-33.442	139.104
N34	N	N	Y	Y	M	OR	2015	14	-33.442	139.104
N30	Y	Y	Y	Y	M	OR	2015	14	-33.441	139.103
N33	N	N	Y	Y	M	OR	2015	14	-33.441	139.103
N42	N	N	Y	Y	M	OR	2016	14	-33.439	139.103
N49	N	N	Y	Y	M	OR	2016	14	-33.439	139.101
N44	Y	Y	N	N	F	OR	2016	14	-33.439	139.101
N21	Y	N	Y	Y	M	OR	2015	14	-33.411	139.111
N40	Y	Y	Y	Y	M	OR	2015	14	-33.411	139.111
N25	Y	Y	Y	Y	M	OR	2015	14	-33.410	139.095
N24	N	N	Y	Y	M	OR	2015	14	-33.410	139.096
N29	N	N	Y	Y	M	OR	2015	14	-33.411	139.112
N39	N	N	Y	Y	M	OR	2015	14	-33.411	139.111
N26	N	N	Y	Y	M	OR	2015	14	-33.411	139.102
N22	N	N	Y	Y	M	OR	2015	14	-33.411	139.103
N23	N	N	Y	Y	M	OR	2015	14	-33.412	139.098
N37	N	N	Y	Y	M	OR	2015	14	-33.442	139.101
N31	N	N	Y	Y	M	OR	2015	14	-33.442	139.107
N38	N	N	Y	Y	M	OR	2015	14	-33.444	139.103
R58759	N	Y	N	N	M	OR	2004	14	-33.434	139.079
R53529	N	Y	N	N	NA	OR	1999	14	-33.345	139.261
R41362	Y	N	N	N	NA	OR	1992	NA	-33.350	139.103
R56417	Y	N	N	N	NA	OR	2001	NA	-33.234	138.250
R41167	Y	N	N	N	M	OR	1992	NA	-33.200	139.619
R41638	Y	N	N	N	F	OR	1992	NA	-33.124	139.196
R41771	Y	N	N	N	NA	OR	1992	NA	-33.061	139.831
BS377	Y	N	N	N	F	OR	2011	NA	-32.095	140.274
BS378	Y	N	N	N	M	OR	2011	NA	-32.095	140.274
BS379	Y	N	N	N	M	OR	2011	NA	-32.094	140.274
R60607	Y	N	N	N	F	OR	2005	NA	-32.067	140.333
BS398	Y	N	N	N	M	OR	2011	NA	-31.981	140.208
BS400	Y	N	N	N	F	OR	2011	NA	-31.981	140.210
TG02	Y	N	N	N	M	SFR	2015	NA	-	-
TGG1	Y	N	N	N	M	SFR	2015	NA	-	-
TGO1	Y	N	N	N	M	SFR	2015	NA	-	-
TGOY1	Y	N	N	N	M	SFR	2015	NA	-	-
TGY1	Y	N	N	N	M	SFR	2015	NA	-	-
TG_F8	Y	N	N	N	F	SFR	2010	NA	-	-
R31224	Y	N	N	N	NA	SFR	1987	NA	-32.867	139.933
MR595	Y	N	N	N	M	SFR	2012	NA	-32.843	138.053
MR588	Y	N	N	N	M	SFR	2012	NA	-32.842	138.057
MR590	Y	N	N	N	M	SFR	2012	NA	-32.842	138.057

MR591	Y	N	N	N	M	SFR	2012	NA	-32.842	138.057
AG63	Y	N	N	N	F	SFR	2010	NA	-32.745	138.073
R41137	Y	N	N	N	NA	SFR	1992	NA	-32.592	139.861
DP88	Y	N	N	N	M	SFR	2010	NA	-32.416	137.993
DS141	Y	N	N	N	F	SFR	2010	NA	-32.310	137.980
WG136	Y	N	N	N	F	SFR	2010	NA	-32.188	138.011
WG143	Y	N	N	N	M	SFR	2010	NA	-32.188	138.010
WG166	Y	N	N	N	M	SFR	2010	NA	-32.188	138.009
WG80	Y	N	N	N	M	SFR	2010	NA	-32.188	138.009
WG135	Y	N	N	N	F	SFR	2010	NA	-32.188	138.011
WG146	Y	N	N	N	M	SFR	2010	NA	-32.187	138.008
WG145	Y	N	N	N	M	SFR	2010	NA	-32.186	138.008
YC58	Y	N	N	N	NA	SFR	2010	NA	-31.958	138.377
YC59	Y	N	N	N	M	SFR	2010	NA	-31.958	138.377
YC60	Y	N	N	N	M	SFR	2010	NA	-31.956	138.372
YC127	Y	N	N	N	M	SFR	2010	NA	-31.956	138.372
YC93	Y	N	N	N	M	SFR	2010	NA	-31.956	138.372
YC110	Y	N	N	N	M	SFR	2010	NA	-31.954	138.375
YC104	Y	N	N	N	M	SFR	2010	NA	-31.953	138.374
YC105	Y	N	N	N	F	SFR	2010	NA	-31.953	138.374
R57145	Y	N	N	N	M	SFR	-	NA	-31.938	138.105
R60917	Y	N	N	N	NA	SFR	2005	NA	-31.625	138.594
W_M31	Y	N	N	N	M	SFR	2010	NA	-31.546	138.603
W_M23	Y	N	N	N	M	SFR	2010	NA	-31.538	138.599
W_M22	Y	N	N	N	M	SFR	2010	NA	-31.538	138.599
BG51	Y	N	N	N	M	SFR	2010	NA	-31.418	138.558
R52282	Y	N	N	N	NA	SFR	1999	NA	-31.395	138.811
A535	Y	N	N	N	M	SFR	2012	NA	-31.281	138.582
A529	Y	N	N	N	M	SFR	2012	NA	-31.280	138.583
A504	Y	N	N	N	M	SFR	2012	NA	-31.280	138.584
A510	Y	N	N	N	F	SFR	2012	NA	-31.279	138.591
A518	Y	N	N	N	M	SFR	2012	NA	-31.279	138.593
A47	Y	N	N	N	M	SFR	2010	NA	-31.277	138.599
R52684	Y	N	N	N	NA	NFR	1999	NA	-30.768	138.707
R51819	Y	N	N	N	M	NFR	1998	NA	-30.611	138.803
R52317	Y	N	N	N	NA	NFR	1999	NA	-30.598	139.133
R52909	Y	N	N	N	NA	NFR	1999	NA	-30.428	139.145
R31653	Y	N	N	N	NA	NFR	1987	NA	-30.267	139.283
R51794	Y	N	N	N	NA	NFR	1998	NA	-30.198	139.233
R52948	Y	N	N	N	M	NFR	1999	NA	-30.121	139.399

876

877 **Table S2.** Sampling sites along a north-south linear transect through the *C. decresii* contact
878 zone. Distance is kilometres (km) from southernmost site 1. Variation (mean ± SD) and samples
879 numbers (*N*) for each trait: hybrid index (H_{Index}; Bayesian *q*-value), mtDNA haplotype, quantum
880 catch of the ultraviolet wavelength sensitive receptor (QC_{UVS}), PC1 scores for throat coloration
881 (T_{PC1}) and dorsolateral phenotype (D_{PC1}).

882

Ancestry	Site	Dist.	H_{Index}	*N*	mtDNA	*N*	QC_{UVS}	T_{PC1}	*N*	D_{PC1}	*N*
South	1	0	0.98 ± 0.06	10	1.0	10	0.65 ± 0.21	0.86 ± 0.08	22	1.65 ± 0.83	32
South	2	14	0.95 ± 0.13	11	1.0	1	0.53 ± 0.14	0.76 ± 0.11	19	1.89 ± 0.90	21
Admixed	3	28	0.44 ± 0.04	11	0.18	6	0.14 ± 0.11	0.30 ± 0.22	15	-0.12 ± 0.51	18
Admixed	4	31	0.40 ± 0.05	31	0.0	10	0.22 ± 0.16	0.48 ± 0.19	37	-0.19 ± 0.80	51
Admixed	5	35.5	0.33 ± 0.06	10	0.0	6	0.08 ± 0.06	0.24 ± 0.21	11	-0.79 ± 0.62	11
Admixed	6	39.5	0.24 ± 0.04	12	0.0	3	0.19 ± 0.12	0.43 ± 0.23	19	-0.22 ± 0.60	19
Admixed	7	45.5	0.16 ± 0.03	9	0.0	1	0.09 ± 0.08	0.23 ± 0.27	6	-0.39 ± 0.54	6
Admixed	8	50.5	0.16 ± 0.05	7	0.0	4	0.09 ± 0.03	0.14 ± 0.01	2	-0.92 ± 0.56	2
North	9	58	0.09 ± 0.01	16	0.0	5	0.18 ± 0.14	0.35 ± 0.21	24	-0.59 ± 0.55	24
North	10	71	0.05 ± 0.01	2	0.0	1	0.10 ± 0.04	0.46 ± 0.09	3	-0.89 ± 0.58	3
North	11	81	0.04 ± 0.02	9	0.0	4	0.18 ± 0.14	0.42 ± 0.12	10	-0.89 ± 0.56	10
North	12	94	0.02 ± 0.02	8	0.0	9	0.28 ± 0.03	0.53 ± 0.02	4	-1.18 ± 0.43	4
North	13	140	0.004 ± 0.02	6	0.0	8	0.20 ± 0.12	0.35 ± 0.22	13	-0.70 ± 0.57	13
North	14	160	0.004 ± 0.003	7	0.0	6	0.20 ± 0.14	0.50 ± 0.18	19	-1.28 ± 0.36	19
			Total	149	-	74	-	-	204	-	233

883

884 **Table S3**. STRUCTURE results summarised in STRUCTUREHARVESTER using the
885 Evanno method for the full dataset of 1333 loci. The selected value of K (number of
886 populations) is denoted with an asterisk.

887

K	Reps	Mean LnP(K)	Stdev LnP(K)	Ln'(K)	|Ln"(K)|	Delta K
1	10	-96935.67	0.590361	—	—	—
2*	10	-85534.28	4.320	11401.39	8426.593	1950.583
3	10	-82559.483	9.957	2974.797	2381.325	164.040
4	10	-81973.575	837.453	589.69	631.141	0.754
5	10	-80752.744	369.785	1220.831	—	—

888

889

890 **Table S4**. Pairwise F_{ST} values between populations [Northern Flinders Ranges (NFR),
891 Southern Flinders Ranges (SFR), Olary Ranges (OR), Contact Zone (CZ), Mainland South
892 (MS), and Kangaroo Island (KI)]. All values are significant at $P < 0.001$.

893

	NFR	SFR	OR	CZ	MS	KI
NFR	-	-	-	-	-	-
SFR	0.173	-	-	-	-	-
OR	0.211	0.027	-	-	-	-
CZ	0.216	0.089	0.058	-	-	-
MS	0.468	0.374	0.355	0.203	-	-
KI	0.571	0.434	0.293	0.293	0.213	-

894

Table S5. Results of throat and dorsolateral phenotype analyses on wild-caught males and captive-bred offspring (both sexes for throat and only males for dorsolateral). Contributions of variables to components in principal component analyses (PC1, PC2), linear discriminant analyses (LD1, LD2) analyses, and results of a *t*-test *(T, P*) between northern and southern lineages. Throat variables are the proportions of orange, yellow, and blue colours on the throat, and the quantum catch of the UV receptor (QC_{UVS}). Dorsolateral variables are the proportions of orange and yellow colours on dorsal surface, and the number of distinct breaks in the lateral stripe at the neck.

	Population	Variable	PC1	PC2	LD1	LD2	*T*	*P*
Throat	Wild-Caught	Orange	54.56	0.82	0.32	-0.82	-5.77	*<0.001*
		Yellow	9.54	69.77	0.09	-0.06	-1.49	0.137
		Blue	35.9	29.41	2.36	-0.78	23.56	*<0.001*
		QC_{UVS}	-	-	0.62	0.6	9.34	*<0.001*
	Captive-Bred	Orange	-	-	-0.09	-0.5	-4.26	*<0.001*
		Yellow	-	-	-0.54	-0.82	-5.69	*<0.001*
		Blue	-	-	0.59	-0.82	2.27	*0.04*
		QC_{UVS}	-	-	1.15	-0.39	8.82	*<0.001*
Dorsolateral	Wild-Caught	Orange	50.06	0.78	0.65	-0.12	-8.75	*<0.001*
		Yellow	0.01	98.21	0.11	1.13	-3.87	*<0.001*
		LS Breaks	49.94	1.01	1.38	0.04	-30.19	*<0.001*
	Captive-Bred	Orange	-	-	-0.29	-1.1	0.81	0.44
		Yellow	-	-	-0.34	0.57	2.53	0.04
		LS Breaks	-	-	-1.3	0.1	19.45	*<0.001*

Table S6. Parameter estimates for 95% confidence sets (cumulative Akaike weight $w_i \leq 0.95$) of best-ranked cline models fitted using *HZAR* for the hybrid index based on 1333 loci (H_{index}), mtDNA haplotype frequencies (mtDNA), PC1 for dorsolateral phenotype (D_{PC1}), quantum catch of the UV wavelength sensitive receptor (QC_{UVS}), and PC1 for throat coloration (T_{PC1}). Cline centre (c) is the distance (km) from the southern-most sampling site, width (w) is 1/slope, *pmin* and *pmax* are frequencies at cline ends (for genetic loci), μR and μL are mean trait values at cline ends (for quantitative traits), δ and τ are tail parameters (right, left, or mirror; distance from cline centre to tail and tail slope, respectively). Two log-likelihood unit support limits for centre and width are shown as 'low' and 'high'. Akaike weight (w_i) shown has been recalculated based on only the 95% confidence set to sum to 1.

Trait	Model	c	c_{low}	c_{high}	w	w_{low}	w_{high}	p_{min} / μ_R	p_{max} / μ_L	δ_L	τ_L	δ_R	τ_R	δ_M	τ_M	AIC_c	w_i
H_{index}	*pmin*/*pmax* observed, no tails	29.47	23.96	33.92	38.55	24.60	62.00	0.00	0.98	-	-	-	-	-	-	8.18	0.23
	pmin/*pmax* observed, right tail	27.74	20.09	32.12	15.65	3.45	45.15	0.00	0.98	-	-	0.31	0.40	-	-	8.47	0.20
	pmin/*pmax* fixed, no tails	29.00	23.16	33.66	42.59	29.15	66.34	0.00	1.00	-	-	-	-	-	-	8.82	0.17
	pmin/*pmax* fixed, right tail	27.04	20.25	32.17	20.51	10.02	49.76	0.00	1.00	-	-	0.97	0.48	-	-	8.93	0.16
	pmin/*pmax* fixed, mirror tails	28.78	24.15	32.93	32.07	4.90	57.43	0.00	1.00	-	-	-	-	14.43	0.40	10.73	0.07
	pmin/*pmax* estimated, no tails	28.32	23.60	33.32	32.44	14.77	56.92	0.03	1.00	-	-	-	-	-	-	11.07	0.05
	pmin/*pmax* observed, mirror tails	29.45	24.49	33.40	31.63	2.13	57.06	0.00	0.98	-	-	-	-	15.68	0.42	11.16	0.05
	pmin/*pmax* observed, left tail	29.49	23.95	33.92	38.46	24.61	61.93	0.00	0.98	133.57	0.94	-	-	-	-	12.38	0.03
	pmin/*pmax* observed, both tails	26.46	21.51	32.17	16.58	5.11	45.45	0.00	0.98	35.23	0.44	0.31	0.42	-	-	12.87	0.02
	pmin/*pmax* estimated, right tail	27.16	22.46	31.99	20.02	7.81	46.24	0.01	0.98	-	-	0.22	0.51	-	-	13.07	0.02

	Weighted Average	**28.41**	**22.37**	**33.00**	**29.77**	**15.05**	**55.84**	**0.00**	**0.99**	**4.52**	**0.036**	**0.23**	**0.10**	**1.75**	**0.05**	**-**	**-**
mtDNA	*pmin*/*pmax* observed, no tails	27.70	14.75	28.17	0.80	0.02	21.88	0.00	1.00	-	-	-	-	-	-	4.17	0.29
	pmin/*pmax* fixed, no tails	27.96	14.76	28.12	0.11	0.07	21.80	0.00	1.00	-	-	-	-	-	-	4.17	0.29
	pmin/*pmax* fixed, right tail	27.60	14.29	28.15	1.03	0.17	21.79	0.00	1.00	-	-	47.72	0.81	-	-	4.17	0.29
	pmin/*pmax* observed, right tail	27.68	13.41	28.17	0.86	0.02	21.89	0.00	1.00	-	-	103.41	0.67	-	-	8.58	0.03
	pmin/*pmax* observed, left tail	27.94	14.74	28.17	0.16	0.01	21.88	0.00	1.00	77.57	0.71	-	-	-	-	8.58	0.03
	pmin/*pmax* fixed, left tail	27.76	14.81	28.14	0.62	0.05	21.86	0.00	1.00	27.18	0.59	-	-	-	-	8.58	0.03
	pmin/*pmax* observed, mirror tails	27.75	14.74	28.17	0.67	0.03	21.87	0.00	1.00	-	-	-	-	47.82	0.28	8.58	0.03
	Weighted Average	**27.78**	**14.59**	**28.17**	**0.64**	**0.08**	**21.85**	**0.00**	**1.0**	**3.35**	**0.04**	**17.20**	**0.26**	**1.53**	**0.01**	**-**	**-**
D_{PC1}	mean/variance estimated, right tail	22.90	16.44	27.89	6.26	0.79	19.52	-1.11	1.77	-	-	0.76	0.00	-	-	502.71	0.77
	mean/variance estimated, mirror tails	23.43	15.96	26.70	39.49	0.92	60.43	-1.66	2.89	-	-	-	-	9.56	0.07	505.10	0.23
	Weighted Average	**23.02**	**16.33**	**27.61**	**13.97**	**0.82**	**29.02**	**-1.24**	**2.03**	**-**	**-**	**0.59**	**0.00**	**2.22**	**0.02**	**-**	**-**
QC_{UVS}	mean/variance observed, no tails	15.85	14.3	18.93	9.04	0.88	16.49	0.20	0.65	-	-	-	-	-	-	-199.63	0.71
	mean/variance estimated, no tail	16.98	14.2	25.99	10.44	0.00	21.58	0.18	0.64	-	-	-	-	-	-	-195.84	0.11
	mean/variance observed, left tail	15.94	14.2	27.16	5.69	0.75	16.96	0.20	0.65	0.47	0.36	-	-	-	-	-195.63	0.10
	mean/variance observed, mirror tails	14.99	14.0	19.17	4.89	0.55	18.67	0.20	0.65	-	-	-	-	4.16	0.84	-195.59	0.09

	Weighted Average	**15.90**	**14.25**	**20.48**	**8.48**	**0.74**	**17.27**	**0.20**	**0.65**	**0.04**	**0.03**	**-**	**-**	**0.39**	**0.08**	**-**	**-**
T_{PC1}	mean/variance estimated, no tails	15.21	15.1	16.11	2.75	2.51	6.58	0.40	0.85	-	-	-	-	-	-	-96.94	0.90
	mean/variance estimated, left tail	16.94	14.7	21.00	7.40	1.78	19.96	0.39	0.86	73.72	0.95	-	-	-	-	-92.58	0.10
	Weighted Average	**15.38**	**15.06**	**16.61**	**3.22**	**2.43**	**7.94**	**0.40**	**0.85**	**7.52**	**0.10**	**-**	**-**	**-**	**-**	**-**	**-**

11

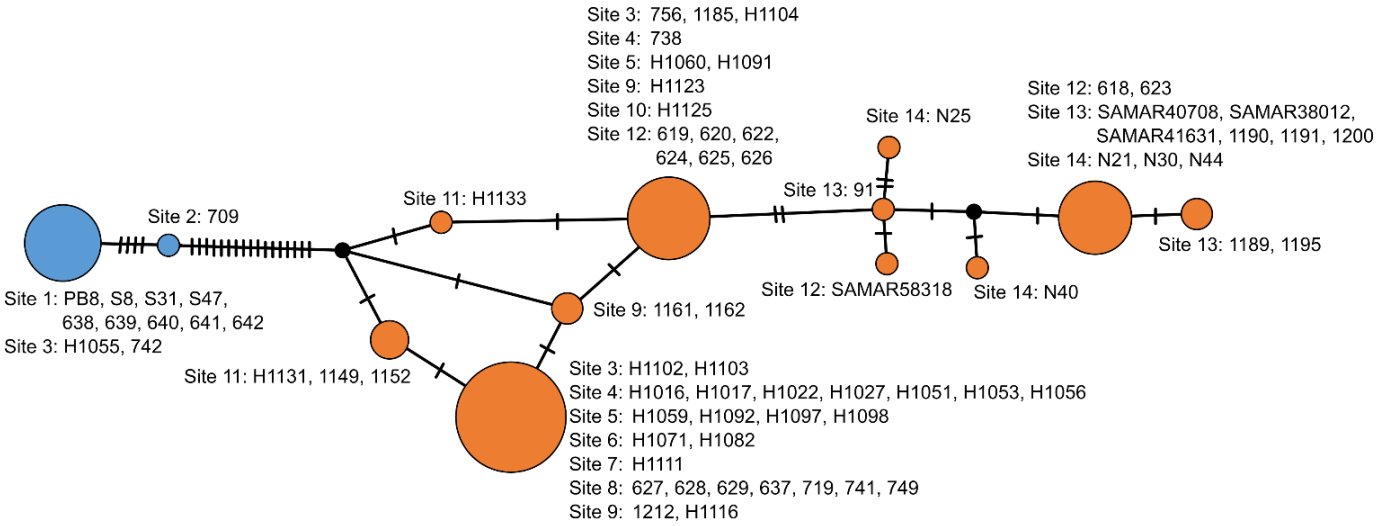

912

913 **Figure S1.** TCS parsimony network of *C. decresii* mtDNA haplotypes constructed from the
914 ND4 region. Circle size corresponds to the frequency of haplotypes and each hash indicates
915 one mutational step. Southern lineage haplotypes are coloured blue, northern lineage
916 haplotypes are orange, and hypothetical missing haplotypes are black. Individuals comprising
917 each circle and their geographic origin (cline site) are indicated by adjacent text.

918

Supplemental Materials and Methods

Captive breeding and offspring rearing

Adult lizards were housed individually in 55 L x 34 W x 38 D cm opaque plastic enclosures containing a layer of sand and two stacked ceramic tiles for shelter and basking. The room was maintained at temperatures and lighting regimes that mimicked natural seasonal variation. During the breeding season, the ambient temperature was 26°C with a 12:12 light:dark light cycle. A heat lamp was provided in each enclosure to generate a thermal gradient and allow animals to attain their preferred body temperature (36°C; Gibbons, 1977; Walker, unpublished data). Lizards were fed live crickets and mealworms *ad libitum* three times per week and misted with water for hydration.

Our breeding design included four possible combinations (northern female x northern male, northern female x southern male, southern female x southern male, southern female x northern male) with up to three 'rounds' of mating to produce multiple clutches in one breeding season. Female enclosures contained a nest box in the form of a clear plastic container 17 x 13 x 15 cm LxWxD with in a 3.5 cm circular entrance in the lower corner, filled with a moist 50:50 sand:peat moss mixture sloped upwards to the top of the box. Eggs were collected following oviposition and incubated in sealed plastic containers filled two-thirds with moist vermiculite (volume ratio 5:1 vermiculite:water) and incubated at 28°C (± 0.12°C) until hatching for a 50:50 sex ratio (Harlow, 2000). Hatchling lizards were housed individually in 30 x 20 x 10 cm plastic enclosures with fly screen lids. Each enclosure contained two stacked ceramic tiles to provide shelter, paper substrate, water dish, heat lamp and UV lighting. Lizards were fed crickets *ad libitum* and misted with water daily.

Confirmation of paternity

Maternity was known for all offspring, however paternity was not known due to multiple mates, and the potential for sperm storage and multiple paternity within clutches in the genus *Ctenophorus* (Hacking, Stuart-Fox, & Gardner, 2017; Lebas, 2001; Olsson, Schwartz, Uller, & Healey, 2007, 2009; Uller, Schwartz, Koglin, & Olsson, 2013). We collected blood from all by venipuncture from the sinus angularis in the corner of the mouth. Genomic DNA was extracted from blood using an E.Z.N.A. Tissue DNA Kit (Omega Bio-tek, Norcross, GA, USA) and sent to the Australian Genome Research Facility (Melbourne, Victoria, AUS) for PCR amplification, fragment visualization and size calling. Paternity was

assigned with a 95% confidence level using a maximum likelihood approach in CERVUS v 3.0.7 (Kalinowski, Taper, & Marshall, 2007; Marshall, Slate, Kruuk, & Pemberton, 1998). First, we conducted a simulation of parentage analysis with the parameters of 50,000 offspring, 1% error rate, 5 candidate fathers, 95% of loci typed, and a minimum of 4 loci typed. Following this, we conducted a paternity analysis based on the trio (mother, father, and offspring) LOD score and a strict 95% confidence level (following Rankin, McLean, Kemp, & Stuart-Fox, 2016). These were manually verified across known breeding pairings.

Testosterone-induced throat colour expression

Crystalline testosterone powder (no. T1500, Sigma) was mixed with sesame oil at a concentration of 0.025 g/mL oil and 4.5 uL of this mixture was pipetted onto the dorsal surface daily for six weeks until throat coloration was apparent (Rankin et al., 2016). Ventral and dorsal photos and spectral measurements of throat coloration were taken weekly.

References

Gibbons, J. R. H. (1977). *Comparative ecology and behaviour of lizards of the* Amphibolurus decresii *species complex*. PhD dissertation. The University of Adelaide.

Hacking, J., Stuart-Fox, D., & Gardner, M. (2017). Very low rate of multiple paternity detected in clutches of a wild agamid lizard. *Australian Journal of Zoology*, *65*(5), 328–334. doi:10.1071/ZO18006

Harlow, P. S. (2000). Incubation Temperature Determines Hatchling Sex in Australian Rock Dragons (Agamidae: Genus *Ctenophorus*). *Copeia*, *4*, 958–964. doi:https://doi.org/10.1643/0045-8511(2000)000[0958:ITDHSI]2.0.CO;2

Kalinowski, S. T., Taper, M. L., & Marshall, T. C. (2007). Revising how the computer program CERVUS accommodates genotyping error increases success in paternity assignment. *Molecular Ecology*, *16*(5), 1099–1106. doi:10.1111/j.1365-294X.2007.03089.x

Lebas, N. R. (2001). Microsatellite determination of male reproductive success in a natural population of the territorial ornate dragon lizard, *Ctenophorus ornatus*. *Molecular Ecology*, *10*(1), 193–203. doi:10.1046/j.1365-294X.2001.01174.x

Marshall, T. C., Slate, J., Kruuk, L. E. B., & Pemberton, J. M. (1998). Statistical confidence for likelihood-based paternity inference in natural populations. *Molecular Ecology*, *7*, 639–655.

Olsson, M., Schwartz, T., Uller, T., & Healey, M. (2007). Sons are made from old stores: sperm storage effects on sex ratio in a lizard. *Biology Letters*, *3*(5), 491–493. doi:10.1098/rsbl.2007.0196

985 Olsson, M., Schwartz, T., Uller, T., & Healey, M. (2009). Effects of sperm storage and male
986 colour on probability of paternity in a polychromatic lizard. *Animal Behaviour*, *77*(2),
987 419–424. doi:10.1016/j.anbehav.2008.10.017

988 Rankin, K. J., McLean, C. A., Kemp, D. J., & Stuart-Fox, D. (2016). The genetic basis of
989 discrete and quantitative colour variation in the polymorphic lizard, *Ctenophorus*
990 *decresii*. *BMC Evolutionary Biology*, *16*(1), 1–14. doi:10.1186/s12862-016-0757-2

991 Uller, T., Schwartz, T., Koglin, T., & Olsson, M. (2013). Sperm storage and sperm
992 competition across ovarian cycles in the dragon lizard, *Ctenophorus fordi*. *Journal of*
993 *Experimental Zoology*, *319A*, 404–408. doi:10.1002/jez.1803

994